





25 being the most abundant. The stratigraphic distribution of the bioclimatic groups  
26 (hydrophytes, hygrophytes, lowland tropical flora, upland flora, and xerophytes)  
27 allowed for the identification of climatic phases: pre-evaporitic, evaporites, and post-  
28 evaporites. In the pre-evaporitic phase, the most significant abundances were between  
29 the hygrophytes and upland flora, indicating a certain level of humidity. Xerophytes  
30 were the most abundant in all phases, with a conspicuous increase in the evaporitic  
31 phase, reflecting an increase in aridity. In the post-evaporitic phase, there was a  
32 significant increase in the upland flora with the return of wetter conditions. This study  
33 confirmed an increasing humidity trend in the analyzed sections, probably owing to the  
34 influence of the Intertropical Convergence Zone that already operated during the late  
35 Aptian.

36

## 37 **1. Introduction**

38 The palynoflora preserved in the upper Aptian rocks of South America and Africa  
39 is typical of hot conditions and is commonly associated with arid climates (Chumakov  
40 et al., 1995, Hay and Floegel, 2012). However, because biodiversity tends to be higher  
41 in wetter climates, the high diversity observed during the Aptian raises the possibility  
42 that this arid phase fluctuated during that period. The palynoflora related to hot and  
43 humid climates exhibits a growing trend toward these conditions, even during the  
44 Aptian. This trend may be linked to the shifting and strengthening of a humid belt  
45 associated with the Intertropical Convergence Zone (ITCZ) (Hay and Floegel, 2012;  
46 Scotese, 2016; Carvalho et al., 2022; Santos et al., 2022), as well as to the establishment  
47 of the South Atlantic, which affected the marine current system.



48 Palynology is a valuable tool for inferring paleoclimatic conditions based on  
49 palynomorph studies. Late Aptian rocks from Brazilian sedimentary basins, including  
50 the Bragança and Codó formations, contain a significant representation of conifers from  
51 the family Cheirolepidiaceae and their pollen grains, such as *Classopollis* (Regali et al.,  
52 1974; Carvalho et al., 2017, 2019, 2022). *Classopollis* is typically associated with arid  
53 conditions, often found in lagoons and coastal areas, and frequently associated with  
54 evaporites (Batten, 1975; Vakhrameev, 1970, 1981; Doyle et al., 1982; Hashimoto,  
55 1995; Heimhofer et al., 2008, Carvalho et al., 2019). However, studies of the Sergipe  
56 Basin (northwestern Brazil), suggest strong fluctuations in the abundance of  
57 *Classopollis* and other xerophytic flora, with a decreasing trend toward the late Aptian  
58 accompanied by an increase in fern spores that require water for reproduction (Carvalho  
59 et al., 2017, 2019). The geographic extent of these trends remains controversial, and  
60 further investigation is required to identify possible climatic oscillations in other  
61 sedimentary basins in Brazil. Analysis of the Codó and Bragança formations, located in  
62 the Cretaceous section of the São Luís, Bragança-Viseu, and Parnaíba basins near the  
63 paleoequator, where the Intertropical Convergence Zone (ITCZ) occurs, has great  
64 potential to provide insights into this topic.

65 The objective of this study was to infer the paleoclimate of the late Aptian period  
66 in the Bragança-Viseu, São Luís, and Parnaíba basins, all located in equatorial areas  
67 (Fig. 1), by examining the relationships between groups of palynomorphs. Furthermore,  
68 this study aimed to investigate how variations in the composition of paleofloras and  
69 indicator species are linked to climatic changes such as shifts in humidity and  
70 temperature, as well as other paleoenvironmental forcings.

71

72



73 **2. Geological settings**

74 According to Milani et al. (2007), the three sedimentary basins considered in this  
75 study are grouped into large assemblies based mainly on the tectonic context in which  
76 they developed: Mesozoic aborted rift basins (Bragança-Viseu and São Luís basins) and  
77 Paleozoic Synclises (Parnaíba Basin).

78 The Bragança-Viseu, São Luís, and Parnaíba basins show a similar stratigraphic  
79 evolution. The Bragança-Viseu and São Luís basins are located on the equatorial margin  
80 and the Parnaíba Basin in north-central Brazil (Fig. 1). The basins constitute a rift  
81 system (graben and semi-graben) located between the terrains of the folding belt.  
82 Together, these cover an area of approximately 645,000 km<sup>2</sup>. The sedimentary  
83 succession of the basins consists of Paleozoic, Mesozoic, and Cenozoic rocks. The  
84 Cretaceous strata are represented by the Bragança (Bragança-Viseu and São Luís  
85 basins), Grajaú, Codó, and Itapecuru Formations. In the studied sections, the Bragança  
86 (EGST-01 and VN-01 wells) and Codó (CI-01, PR-01, PE-01, RL-01 wells) formations  
87 were recognized.

88 The Bragança Formation consists of gray medium- to coarse-grained sandstones  
89 and conglomerates supported by conglomerates and greenish siltstones. This formation  
90 is interpreted as an alluvial fan deposit.

91 The Codó Formation is composed of dark shales, anhydrite, and calcilutites, with  
92 sandstone intercalations. These deposits were assigned to a lagoonal environment.  
93 Marine incursions are indicated by fossil contents and the occurrence of evaporitic  
94 deposits.

95

96



### 97 **3. Late Aptian climatic evolution**

98           The pre-evaporitic, evaporitic, and post-evaporitic phases are recognized for the  
99 late Aptian. These phases occur within the K40-K50 supersequences, and show an  
100 average maximum thickness of approximately 650 m in the studied basins. The pre-  
101 evaporitic phase is represented by carbonate and siliciclastic deposits formed in fluvial  
102 and lacustrine deltaic environments within a large proto-oceanic gulf (Milani et al.,  
103 2007). The peak of the evaporitic deposition is recorded in the K50 supersequence, with  
104 widespread occurrences in the Brazilian equatorial margin. The origin of these deposits  
105 is heat intensification associated with the widening of the Atlantic Ocean. These  
106 conditions caused strong evaporation, leading to a wide distribution of evaporites  
107 (mainly halite and anhydrite gypsum) in the South Atlantic basins. The post-evaporitic  
108 phase is characterized by fully marine conditions, evidenced by the rich assemblages of  
109 marine fossils. During this phase, carbonates were deposited, followed by muddy and  
110 sandy sediments, in shallow marine to slope environments.

111           The Bragança and Codó formations are inserted within the K40-K50 Supersequence.  
112 However, in the Bragança Formation, only the pre-evaporitic phase is recognized. On  
113 the other hand, the Codó Formation has recorded the three climatic phases (pre-  
114 evaporitic, evaporitic, and post-evaporitic).

115

### 116 **4. Material and methods**

117

#### 118 **4.1. Studied sections**

119           This study was based on core samples from three basins: Bragança-Viseu and São  
120 Luís located in the equatorial margin, and the Parnaíba Basin in north-central Brazil.



121 The material for this study was derived from the cores of wells EGST-1 and VN-1 from  
122 the Bragança-Viseu Basin; PR-1, PE-1, and RL-1 from the São Luís Basin; and CI-1  
123 from the Parnaíba Basin (Table 1), all drilled by Petrobras (the Brazilian oil company)  
124 (Fig. 1). Detailed information on the studied sections is presented in Table 1.

125 The stratigraphic succession studied comprises parts of the Bragança-Viseu, São Luís,  
126 and Parnaíba Basins. The Bragança-Viseu Basin includes wells EGST-1 (676-1872.1 m),  
127 consisting of sandstones, siltstones, and conglomerates, and VN-1 (1287.6-1317.69 m),  
128 consisting only of sandstones (Fig. 2) (Table 1).

129 Three sections are from the São Luís Basin: PR-1 (1507.6-1513.1 m), composed of  
130 sandstones and siltstones, and PE-1 (1562-1776.8 m), which has a lithology similar to  
131 that of the previous one, with the addition of calcarenites. RL-1 (1157.3-1240.3 m) is  
132 composed of sandstones, siltstones, calcarenites, and anhydrites. The fourth section, CI-  
133 1 (768-907.1 m), is from the Parnaíba Basin. CI-1 has a lithology similar to that of RL-1,  
134 but the former has a more pronounced package of anhydrites than the latter does (Fig. 2)  
135 (Table 1).

136 The late Aptian age of the samples is based on the *Sergipea variverrucata*  
137 Biozone recognized in two studied drill cores (PR-1 and CI-1), which is correlated with  
138 part of the upper Aptian *Globigerinelloides algerianus* Zone (Carvalho et al., 2016). In  
139 the other four sections (EGST-1, VN-1, PE-1, and RL-1), *Sergipea variverrucata* was  
140 not recognized. However, the identified floristic associations (e.g., *Afropollis jardinus*,  
141 *Araucariacites australlis*, *Bennettitapollenites regallie*, *Equisetosporites maculosus*,  
142 *Klukisporites foveolatus*, *Sergipea simplex*) are attributed to the late Aptian of Brazil  
143 (Regali and Santos, 1999; Carvalho et al., 2017, 2019).

144

145



146 **4.2. Sample preparation**

147 The samples were prepared at the Research and Development Center of Petrobras  
148 (CENPES) in Rio de Janeiro. The method used was the standard Petrobras method of  
149 palynological preparation compiled by Uesugui (1979) on the basis of methods  
150 developed by Erdtman (1943, 1969) and Faegri et al. (1966). Thus, in this study, most  
151 mineral constituents were dissolved by hydrochloric and hydrofluoric acids before  
152 heavy-liquid separation, and the remaining organic matter was sieved through a 10 µm  
153 mesh before mounting on slides.

154

155 **4.3. Palynological analyses**

156 The samples were analyzed using a transmitted light microscope. Analysis was  
157 based on the first 200 palynomorphs counted on each slide. The marine elements  
158 (dinoflagellate cysts and microforaminiferal linings) were counted separately.  
159 Taxonomic identification was based on the methods of Regali et al. (1974), Lima  
160 (1978), Dino (1992, 1994), and Carvalho et al. (2019, 2022).

161

162 **4.4. Bioclimatic analysis**

163 Palynomorphs are useful climatic indicators (bioclimatic groups) because of their  
164 botanical affinities. However, identifying the spores and pollen grains of the parent  
165 plant classified at the family level is often challenging. This study referred to the  
166 literature (e.g., Dino, 1994; Carvalho, 2004; Souza-Lima and Silva, 2018; Jansonius et  
167 al., 1976-1996) to identify the botanical affinities of the indicator species.



168           On the basis of botanical affinities and inferred paleoenvironmental conditions,  
169 this study proposes five bioclimatic groups: hydrophytes, hygrophytes, tropical lowland  
170 flora, upland flora, and xerophytes. These groups provide valuable insights into the  
171 climate and vegetation of the study area.

172

#### 173 **4.5. Wet-dry trend**

174           To support the bioclimatic group distribution, we used the Fs/X (fern spores  
175 *versus* xerophytes) ratio. This ratio is based on the co-occurrence of fern spores and  
176 xerophytic palynomorphs (*Classopollis* and polyplicate gnetalean pollen); therefore, it  
177 can be used as an indicator of dry-wet trends (Carvalho et al., 2019). The ratio of fern  
178 spores to xerophytic palynomorphs (Fs/X) was calculated as  $Fs/X = nFs / (nFs + nX)$ ,  
179 where n is the number of specimens counted, Fs is the number of fern spores (non-  
180 reworked), and X is the number of xerophytic pollen grains. In summary, Fs/X  
181 approaching 1 implies high humidity, and that approaching -1 indicates low humidity.

182

#### 183 **4.6. Diversity**

184           Shannon-Weaver diversity indices H (S) were calculated for all samples by using  
185 PAST software (Hammer et al., 2001) to provide information for interpreting  
186 paleoclimatic trends. Diversity H(S) considers the abundance of each species and is  
187 used to characterize the diversity of the assemblages.

188

189

190





#### 191 **4.7. Indicator species**

192 To reconstruct the late Aptian vegetation in the studied basins, we employed the  
193 indicator species analysis (IndVal) method. This index was applied for the first time in  
194 pre-Quaternary samples in the der Sergipe Basin (Carvalho et al., 2017).

195 The IndVal index determines the taxa strongly associated with particular groups  
196 of samples and is assumed to reflect the climatic conditions of those groups. It was  
197 calculated using the formula proposed by Dufrêne and Legendre (1997):  $\text{IndValGroup}$   
198  $k, \text{Species } j = 100 \times A_{k,j} \times B_{k,j}$ , where  $A_{k,j}$  represents specificity, and  $B_{k,j}$  represents  
199 fidelity. We used PAST software (Hammer et al., 2001) to calculate these values.

200 To ensure that our IndVal analysis fulfilled the criteria of ordination and climate-  
201 focused approach, we grouped the samples according to three climatic phases: pre-  
202 evaporitic, evaporitic, and post-evaporitic. This allowed us to identify the specific  
203 indicator species associated with each climatic phase and gain insights into the  
204 vegetation that existed during the late Aptian period.

205

#### 206 **5. Results**

207 Sixty-nine genera were identified in the 40 samples and were distributed into five  
208 plant groups: bryophytes (four genera), ferns (17 genera), lycophytes (10 genera),  
209 pteridosperms (one genus), gymnosperms (23 genera), and angiosperms (14 genera)  
210 (Appendix 1) (Table 2). Twenty indeterminate morphotypes were found in ferns and 10  
211 in angiosperms. Of the 69 genera identified, nine occurred in all the wells studied:  
212 *Afropollis*, *Araucariacites*, *Callialasporites*, *Cicatricosisporites*, *Classopollis*,  
213 *Cyathidites*, *Deltoidospora*, *Equisetosporites*, *Verrucosisporites*.



214 The recognition of botanical affinities of the 69 genera was based on the literature  
215 (e.g., Dino 1992, Balme 1995; Antonioli, 2001; Carvalho et al., 2017, Carvalho et al.,  
216 2019, Carvalho et al., 2022) and the database of *fossilworks.org*. The suggested  
217 botanical affinity of the 69 genera was 94.2%. The 5.8% without botanical affinity  
218 refers to the group of angiosperms.

219 All bioclimatic groups were present in the studied sections (Table 3, Appendix 2).  
220 In general, the palynological assemblage is predominantly composed of the xerophytic  
221 bioclimatic group, characterized by a high abundance of *Classopollis*. The average  
222 abundance of xerophytes was 55.7%, ranging from 46.3% to 63.6% in the sections  
223 studied (Table 4). In sequence, the upland flora had an overall average abundance of  
224 18.9% (ranging from 7.8% to 26%), with *Araucariacites* being the dominant taxon. The  
225 hygrophyte bioclimatic group is characterized by the presence of *Cicatricosisporites*,  
226 which had an average abundance of 18.6% (ranging from 11.4% to 28.4%). By contrast,  
227 the hydrophyte bioclimatic group is the least abundant, with an overall average of 0.7%,  
228 and is dominated by the genus *Crybelosporites*. Regarding diversity, the Shannon-  
229 Wiener indices ( $H'$ ) obtained for the 40 samples showed an overall average of  $H' = 2.0$ ,  
230 which ranged from  $H' = 1.6$  in the VN-1 section to  $H' = 2.2$  in section PE-1 (Table 4).  
231 The values of the wet-dry trend (Fs/X ratio) ranged from 0.19 (dry) in section CI-1 to  
232 0.39 (wet) in EGST-1(wet) (Table 4).

233

### 234 **5.1. Stratigraphic distribution of bioclimatic groups in EGST-1 well**

235 Although xerophytes are dominant overall, EGST-1 well exhibits a higher  
236 abundance of hygrophytes (24.9%) due to moderate to high occurrences of  
237 *Cicatricosisporites* and trilete psilate (e.g., *Cyathidites*), especially at the base of the  
238 well (Fig. 3). Additionally, the abundance of hygrophytes, tropical lowland flora, and



239 upland flora increases toward the upper sections, whereas the abundance of xerophytes  
240 decreases (Fig. 4). The Shannon-Wiener indices ( $H'$ ) showed an overall average of  $H'$ =  
241 2.1, slightly above the general average ( $H'$ = 2.0). The  $F_s/X$  ratio had the highest value  
242 for all sections (0.38), above the overall average (0.28), indicating more humid  
243 conditions (Table 4).

244

### 245 **5.2. Stratigraphic distribution of bioclimatic groups in VN-1 well**

246 Similar to the EGST-1 well, the VN-1 well is composed of four samples from the  
247 Bragança Formation, in which xerophytes dominate. However, unlike the former well,  
248 hygrophytes exhibit the highest average abundance (28.4%) among all studied wells,  
249 primarily because of the abundance of trilete psilate. Despite few samples, an increasing  
250 trend of hygrophytes, tropical lowland flora, and upland flora was observed, with a  
251 significant peak in hygrophytes (Fig. 4). The average diversity of  $H'$ =1.6 is the lowest  
252 for the studied basins, below the overall average ( $H'$ = 2.0). The  $F_s/X$  ratio was 0.31,  
253 above the overall average (0.28).

254

### 255 **5.3. Stratigraphic distribution of bioclimatic groups in PR-1 well**

256 The section comprises four samples from the Codó Formation. Notably, the PR-1  
257 well exhibits the lowest average abundance of xerophytes (46.3%) (Table 4). However,  
258 it shows the highest average abundance in the tropical lowland flora group (20.4%) of  
259 all the wells studied, driven by the presence of the genus *Afropollis*. In general, an  
260 increasing trend toward hygrophytes, upland flora, and mainly tropical lowland flora  
261 was observed (Fig. 5). The average diversity was  $H'$ = 2.1 in this well. This value is one  
262 of the highest values among all the wells studied. This high diversity is mainly



263 attributed to the significant number of species belonging to the tropical lowland flora  
264 group. The Fs/X ratio was 0.25, slightly below the overall average (0.28) (Table 4).

265

#### 266 **5.4. Stratigraphic distribution of bioclimatic groups in PE-1 well**

267 The PE-1 well shows a clear decreasing trend upward of the xerophytes, which  
268 did not exceed 20% (Fig. 6). By contrast, hygrophytes and upland flora show a  
269 conspicuous increase. Highlight for the upland flora group show an average of 26%  
270 driven by the genus *Araucariacites*. The average diversity of  $H'=2.2$  is the highest for  
271 the basins. This average diversity is due to the many species of upland flora and  
272 hygrophytes. The Fs/X ratio was 0.28, the same as the overall average (0.28) (Table 4).

273

#### 274 **5.5. Stratigraphic distribution of bioclimatic groups in RL-1 well**

275 The section consists of seven samples from the Codó Formation. The xerophytic  
276 bioclimatic group dominated the entire section, with no sudden changes in the  
277 abundance curve observed, except at the base of the section, where the hygrophytes,  
278 tropical plain flora, and upland flora groups together reached almost 40% (Fig. 7). The  
279 average diversity of  $H'=1.9$  is the second lowest for the studied basins. The Fs/X ratio  
280 was 0.24, slightly below the overall average (0.28) (Table 4).

281

#### 282 **5.6. Stratigraphic distribution of bioclimatic groups in CI-1 well**

283 The Parnaíba Basin is represented by one well, which comprises 13 samples from  
284 the Codó Formation. The palynological assemblage of this section was dominated by  
285 the xerophytic bioclimatic group, with a high average of 63.6%, largely because of the  
286 abundance of *Classopollis* and *Equisetosporites*. The dendrogram shown in Fig. 8  
287 reveals two intervals: the base with a greater balance between xerophytes and the other



288 groups, especially the upland flora (15.9%) (Table 4). The Fs/X ratio recorded the  
289 lowest value in all sections (0.19), which was below the overall average (0.28),  
290 indicating drier conditions (Table 4). However, despite this, the average diversity of  
291  $H'=2.0$  was one of the highest, with the same value as the overall average of 2.0.

292

### 293 **5.7. Climatic phases**

294 All six sections were individually analyzed for palynology. However, a composite  
295 section was constructed (Table 5) based on the stratigraphically evident chronological  
296 distribution of the climatic phases in each studied section. The composite section of the  
297 Bragança-Viseu, São Luís, and Parnaíba basins consists of 40 samples, with 24 samples  
298 from the pre-evaporitic phase, eight from the evaporitic phase, and eight from the post-  
299 evaporitic phase (Table 5). In general, the composite section highlights the bioclimatic  
300 groups of hygrophytes (18.8%) and tropical lowland flora. The diversity and Fs/X ratio  
301 curves showed strong synchrony, indicating a relation between diversity and humidity  
302 (Fig. 9). No marine elements were recorded in these sections.

303 During the pre-evaporitic phase, there is a higher abundance of xerophytes,  
304 hygrophytes, and upland flora, but with strong oscillations observed in their respective  
305 curves. The dendrogram in Fig. 9 identifies two intervals within this phase: with  
306 significant values of xerophytes at the base but with a decreasing trend toward the top.  
307 The interval above the xerophyte curve exhibits an upward trend. The diversity and  
308 Fs/X ratio curves show synchrony but with a decreasing trend toward the top. The  
309 indicator species (IndVal) identified for the pre-evaporitic phase, *Deltoidospora* spp.  
310 (Cyatheaceae-Dicksoniaceae) is related to the montane rainforest, suggesting more  
311 humid conditions (Table 5).



312           The evaporitic phase, which corresponds to the gypsum layers of the Codó  
313 Formation, is characterized by the highest average of the xerophytic bioclimatic group  
314 in the composite section (Table 5). Additionally, the average abundance of the tropical  
315 lowland flora group is also high, driven by the genus *Afropollis*. Surprisingly, the mean  
316 diversity is high during this phase, but the mean Fs/X ratio is the lowest. The high  
317 diversity in arid conditions is due to the great diversity of species in the xerophytic  
318 group, such as *Classopollis classoides*, *Equisetosporites maculosus*, and  
319 *Gnetaceaepollenites jansonius*. The IndVal for the evaporitic phase is *Afropollis* spp.  
320 related to tropical lowland flora (Table 5).

321           The post-evaporitic phase, which includes part of a section of the Codó  
322 Formation, is characterized by a significant decrease in the dominance of the xerophytic  
323 bioclimatic group; lower average abundance (47%) in PR-1; and the clear dominance of  
324 hygrophyte groups, including tropical lowland flora and upland flora. The dendrogram  
325 reveals a break between this phase and the evaporitic phase (Fig. 9). In general, this  
326 reflects an inversion in abundance between groups related to humidity (hygrophytes,  
327 hydrophytes, tropical flora, and upland flora) and groups related to drier conditions  
328 (xerophytes) (Fig. 9). In this phase, the indicator species is *Deltoidospora* spp.,  
329 suggesting more humid conditions for pre- and pro-evaporitic phases.

330

## 331 **6. Discussion**

332           The data obtained from these sections provide clear evidence of the dominance of  
333 the xerophytic bioclimatic group during the late Aptian in Brazilian sedimentary basins.  
334 This information supports that in the literature that suggests an essentially arid climate  
335 during this period (e.g., Lima, 1983; Suguio and Barcelos, 1983; Petri, 1983; Rossetti et



336 al., 2003; Hay and Floegel, 2012, Carvalho et al., 2017, 2019, 2022). These authors  
337 attributed this aridity to the predominance of conifers from the Cheirolepidiaceae family  
338 and their *Classopollis* pollen grains. However, climatic oscillations were identified  
339 during this period, indicated by bioclimatic groups related to the humid conditions:  
340 hydrophytes, hygrophytes, tropical lowland flora, and upland flora. A relationship  
341 between these groups has been suggested (e.g., Carvalho et al., 2017, 2019, 2022). In  
342 this study, principal component analysis (PCA) was conducted between bioclimatic  
343 groups that exhibited patterns similar to those observed in the literature (e.g., Carvalho  
344 et al., 2017, 2019, 2022). The PCA revealed a positive correlation among hygrophytes,  
345 hydrophytes, tropical lowland flora, and upland flora, whereas xerophytes show a  
346 negative relationship on the first axis (Component 1) (Fig. 10), explaining more than  
347 70% of the variation. Component 1 characterizes the wet-dry trend.

348         The sections of the São Luís Basin (PE-1, RL-1, and PR-1) showed the lowest  
349 abundance of xerophytic flora, followed by the sections of the Bragança-Viseu Basin  
350 (VN-1 and EGST-1) and the CI-1 section (Parnaíba Basin) farther south (Fig. 11A).  
351 More humid conditions also were suggested by Santos et al. (2022) for the São Luis  
352 Basin. This study utilized palynological data and PCA analysis to propose the existence  
353 of a wet phase during the late Aptian in the São Luis Basin. Through the analysis of the  
354 abundance of *Araucariacites* and fern spores, as well as the presence of the genus  
355 *Classopollis* associated with carbonate sedimentation in two semi-arid intervals, an  
356 intermediate humid interval was identified. The authors suggested that the data were  
357 sufficient to identify a pre-Albian humid belt, which challenges the view of exclusively  
358 arid Gondwana during the Aptian and supports the presence of a wet phase.

359         As also suggested by Carvalho et al. (2022), we compared the studied sections  
360 with sections in the Espírito Santo Basin, located much farther south (at 20°S). We



361 found that the studied basins had a lower abundance of xerophytic flora than the  
362 Espirito Santo Basin did (Fig. 11B-C). The decreasing trend in aridity observed from  
363 the southeast (Espirito Santo Basin) to the northeast (Fig. 11B-C) coincides with the  
364 location of the hot and humid belt attributed to the ITCZ (Ohba et al., 2010, Chaboureau  
365 et al., 2012, 2014; Scotese, 2016). Notably, the approach to the ITCZ belt, where xeric  
366 restrictions are milder, reflected even in the most aridity phase, the evaporitic phase,  
367 whose indicator species was the *Afropollis* spp. of the lowland tropical flora. This  
368 indicates that the ITZC must have had diminished aridity. The genus *Afropollis* has  
369 been associated with hot, humid climates. According to Carvalho et al. (2022), this  
370 genus exhibits the weakest negative correlation with xerophytic flora (e.g.,  
371 *Classopollis*).

372 The ITCZ belt proposed by Scotese (2016) for the Aptian covers the entire  
373 African continental paleoequator. However, although very close, it did not reach South  
374 America (Fig. 11B). Palynological analyses conducted by Deaf et al. (2020) on the late  
375 Aptian material of the Dahab Formation (Mathruh Basin, Egypt) indicated a  
376 predominance of fern spores from the hygrophyte bioclimatic group (e.g.,  
377 *Triplanosporites*, *Cicatricosisporites*) and uplands (e.g. *Deltoidospora*, *Araucariacites*),  
378 accounting for approximately 60% on average. This finding suggests that the formation  
379 is characterized by humid conditions.

380 The xerophytic flora (*Classopollis* and *Equisetosporites*) in the Dahab Formation  
381 averaged approximately 25%. Considering the climatic belts proposed by Scotese  
382 (2016, 2021), this formation occurred “inside” the ITCZ, which is reflected in the  
383 prevalence of bioclimatic groups associated with more humid conditions. The  
384 abundance of xerophytic flora in the Dahab Formation (Mathruh Basin) was lower than  
385 that in the sections studied. This difference was particularly significant when compared





386 with the Espírito Santo Basin, where the abundance of xerophytic flora was 87.3%, as  
387 opposed to 25% in the Dahab Formation (Fig. 11C). Notably, a significant contributor  
388 to the humidity in the Dahab Formation was likely a marine influence, which was not  
389 present in the sections studied.

390

## 391 7. Conclusion

392 The Aptian sections studied have well-preserved palynological diversity  
393 dominated by the genera *Classopollis* (Cheirolepidiaceae) and *Araucariacites*  
394 (Araucariaceae). Some genera of ferns are also abundant such as *Cicatricosisporites*  
395 (Anemiaceae), *Verrucosisporites* (Osmundaceae), and *Deltoidospora* (Cyatheaceae).

396 Five bioclimatic groups were identified and proposed for interpretation:  
397 hydrophytes, hygrophytes, tropical lowland flora, upland flora, and xerophytes. The  
398 bioclimatic groups provide evidence that the climate during the late Aptian was arid.  
399 However, when considering the distribution curves of bioclimatic groups, as well as the  
400 indicator species (IndVal) and diversity, a clear upward trend toward increased humidity  
401 was observed.

402 The late Aptian period was characterized by three distinct climatic phases: pre-  
403 evaporitic, evaporitic, and post-evaporitic. During the pre-evaporitic phase, despite the  
404 dominance of xerophytic flora, there were episodes of humidity, evidenced by indicator  
405 species such as *Deltoidospora* spp. The evaporitic phase was dominated by xeric  
406 elements, although the moderate to high abundance of lowland tropical flora, confirmed  
407 by *Afropollis* spp. as an indicator species, indicated some periods of humidity. The post-  
408 evaporitic phase was marked by a lower abundance of xerophytic elements and a clear



409 dominance of groups associated with wet conditions, mainly the upland flora,  
410 suggesting a wetter climate during this phase.

411 The climatic variation during the late Aptian is reflected in the palynological  
412 assemblages, with the arid phase being dominated by the genus *Classopollis* and other  
413 xerophytic bioclimatic group indicators. The wet phase is marked by a significant  
414 decrease in xerophytes and a high abundance and diversity of *Araucariacites*, fern  
415 spores, and other genera related to highland, hydrophytic, and hygrophytic bioclimatic  
416 groups. The "mirror effect" observed in the frequency curves highlights the ecological  
417 differences between the arid and humid trend groups.

418 According to our findings, vegetation dynamics were affected by a combination of  
419 the Intertropical Convergence Zone (ITCZ) and the opening of the South Atlantic Ocean  
420 during the late Aptian period. The influence of the ITCZ is currently stronger in the  
421 north-central region of South America. Notably, climate evolution during the late  
422 Aptian in the South Atlantic led to increased humidity, which was closely linked to  
423 plant diversity and marine influences.

424

## 425 **Appendices**

426

427

428

429

430



Appendix 1. Eleven plates with the most relevant palynomorphs recorded in the studied wells.

### PLATE 1

- A. *Stereisporites* sp. Pflug, 1953 (RL-1).
- B. *Todisporites* sp. Couper, 1958 (RL-1).
- C. *Deltoidospora diaphana* Wilson & Webster, 1946 (EGST-1).
- D-E. *Deltoidospora minor* (Couper 1953) Pocock 1970<sup>a</sup> (CI-1).
- F. *Cyathidites* sp. Couper, 1953 (CI-1).
- G. *Cyathidites minor* Couper, 1953 (CI-1).
- H. *Biretisporites* sp. Delcourt & Sprumont, 1955 emend. Delcourt, Dettmann & Hughes, 1963 (CI-1).
- I. *Biretisporites Pontoniaei* Delcourt & Sprumont, 1955 (RL-1).
- J. *Undulatisporites* sp.? Thomson & Pflug, 1953 (CI-1).
- K. *Granulatosporites* sp. Ibrahim, 1933 (CI-1).
- L. *Verrucosisporites* sp. Ibrahim, 1933 emend. Potonié & Kremp, 1955 (CI-1).

### PLATE 2

- A. *Leptolepidites psarosus* Norris, 1966 (CI-1).
- B. *Leptolepidites verrucatus* Couper, 1953 (CI-1).
- C-D. *Uvaesporites* sp. Doring, 1965 (CI-1).
- E. *Apiculatisporis* sp. Potonié & Kremp, 1954 (CI-1).
- F. *Echinatisporis* sp. Krtuzsch, 1959 (CI-1).
- G. *Hamulatisporis* sp. Krtuzsch, 1959 (RL-1).
- H. *Cicatricosisporites* sp. Potonié & Gelletch, 1933 (EGST-1).



- I. *Cicatricosisporitesavnimelechi* Horowitz, 1970 (CI-1).
- J-K. *Cicatricosisporites brevilaesuratus* Couper, 1958 (EGST-1).
- L. *Cicatricosisporites cf. Cicatricosisporites?* sp.5 Duarte, 2011 (EGST-1).

### PLATE 3

- A - B. *Lycopodiumsporites* sp. Thiegart, 1938 (RL-1).
- C. *Klukisporites variegatus* Couper, 1958 (CI-1).
- D. *Klukisporites* sp. Couper, 1958 (RL-1).
- E. *Klukisporites foveolatus* Pocock, 1964 (EGST-1).
- F. *Klukisporites pseudoreticulatus* Couper, 1958 (CI-1).
- G. *Foveotriletes* sp. Hammen, 1956 (CI-1).
- H. *Gleicheniidites Senonicus* Ross, 1949 (PR-1).
- I. *Camarozonaesporites* sp. Pant, 1954 ex. Pontonié, 1956 *emend.* Klaus, 1960 (VN-1).
- J. *Antulsporites* sp. Archangelsky & Gamero, 1966 (CI-1).
- K. *Cingulatisporites verrucatus* Regali, Uesugui & Santos, 1974 (PE-1)
- L. *Distaltriangulisporites* sp. Singh, 1971 (RL-1).
- M. *Cingutriletes* Pierce, 196 (PR-1).

### PLATE 4

- A. *Matonisporites silvai* Lima, 1978 (PR-1).
- B-C. *Appendicisporites* sp. Weiland & Krieger, 1953; (PR-1).
- D. *Aequitriadites* sp. Delcourt & Sprumont, 1955 *emend.* Dettmann, 1963 (RL-1).



- E. *Perotrilites* sp. Erdtman, 1947 ex. Couper, 1953 (RL-1).
- F. *Crybelosporites pannuceus* Brenner, 1963 *emend.* Srivastava, 1975 (RL-1)
- G. *Paludites mameolatus* Lima, 1978 (PR-1).
- H. *Densoisporites* sp. Weyland & Krieger, 1953 (EGST-1).
- I. *Triporoletes* sp. Mtchedlishvili, 1960 (RL-1).
- J. *Reticulosporis* sp. Krutzsch, 1959 (PR-1).
- K. *Reticulosporis foveolatus* Krutzsch, 1959 (EGST-1).
- L. *Callialasporites trilobatus* Dev, 1961 (CI-1).

## PLATE 5

- A. *Callialasporites dampiere* Dev, 1961 (CI-1).
- B. *Complicatisaccus cearensis* Regali, 1989c (PR-1).
- C. *Cedripites* sp. Wodehouse, 1933 (CI-1).
- D. *Vitreisporites pustulosus* Regali, 1987 (PR-001-MA); (PE-1).
- E. *Vitreisporites microsaccus* Jersey, 1964 (PR-1).
- F. *Vitreisporites pallidus* Nilsson, 1958 (PR-1).
- G. *Rugubivesiculites bahiasulensis* Pierce, 1961 (RL-1).
- H. *Inaperturopollenites* sp. (Pflug, 1952 ex. Thomsom e Pflug, 1953, Pontonié, 1958) Pontonié, 1966 (RL-1).
- I. *Araucariacites* sp. Cookson, 1947 ex Couper, 1953 (CI-1).
- J. *Araucariacites australis* Cookson, 1947 (CI-1).
- K. *Araucariacites limbatus* (Balme) Habib, 1957 (EGST-1).
- L. *Araucariacites pergranulatus* Volkheimer, 1968 (EGST-1).



## PLATE 6

- A. *Araucariacites* sp. S. Cl. 265 A Jardiné & Magloire, 1965 (EGST-1).
- B. *Balmeopsis* sp.? Archangelsky, 1977 (PE-1).
- C. *Balmeopsis limbatus* Archangelsky, 1977 (EGST-1).
- D. *Cingulatipollenites* sp.? Saad & Ghazaly, 1976 (PE-1).
- E. *Cingulatipollenites aegyptiaca* Saad & Ghazaly, 1976 (EGST-1)
- F. *Spheripollenites* sp. Couper, 1958 (RL-1).
- G. *Spheripollenites scabratus* Couper, 1958 (EGST-1).
- H. *Sergipea variverrucata* Regali, Uesugui & Santos, 1974 *emend.* Regali, 1987 (PR-1).
- I. *Sergipea simplex* Regali, 1987 (PE-1).
- J. *Uesuguiipollenites callosus* Dino, 1992 (RL-1).
- K. *Classopollis classoides* Pflug, 1953 (CI-1).
- L. *Classopollis brasiliensis* Hengreen, 1973 (PE-1).

## PLATE 7

- A. *Equisetosporites aff. elegans* Lima, 1978 (CI-1).
- B. *Equisetosporites dudarensis* (Deák, 1964) Lima, 1980 (CI-1).
- C. *Equisetosporites ambuguus* Hedlund, 1966 (RL-1).
- D. *Equisetosporites consinnus* Singh, 1964 (PR-1).
- E. *Equisetosporites leptomatus* Lima, 1978 (CI-1).
- F. *Equisetosporites luridus* Lima, 1978 (CI-1).
- G. *Equisetosporites lanceolatus* Lima, 1978 (CI-1).
- H. *Equisetosporites aff. leptomatus* Lima, 1978 (CI-1).



- I. *Elateropollenites bicornis* Regali, 1989e (EGST-1).
- J. *Elateropollenites dissimilis* Regali, 1989e (EGST-1).
- K. *Classopollis intrareticulatus* Volkheimer, 1972 (PR-1).
- L. *Equisetosporites aff. luridus* Lima, 1978 (RL-1).

#### PLATE 8

- A. *Equisetosporites maculosus* Dino, 1992 (CI-1).
- B. *Equisetosporites minuticosatus* Lima, 1978 (PR-1).
- C. *Equisetosporites aff. minuticosatus* Lima, 1978 (CI-1).
- D. *Equisetosporites ovatus* (Pierce) Singh, 1961 (CI-1).
- E. *Gnetaceaepollenites* sp. Thiegart, 1938 (CI-1).
- F. *Gnetaceaepollenites consisus* Regali, 1989c (CI-1).
- G. *Gnetaceaepollenites jansonii* Pocock, 1964 (CI-1).
- H. *Gnetaceaepollenites uesuguii* Lima, 1978 (CI-1).
- I. *Gnetaceaepollenites undulatus* Regali, Uesugui & Santos, 1974 (RL-1).
- J. *Steevesipollenites* sp. Stover, 1964 (CI-1)..
- K. *Singhia* sp. Srivastava, 1968 (PR-1).
- L. *Singhia punctata* Lima, 1978 (EGST-1)

#### PLATE 9

- A. *Regalipollenites* sp. Lima, 1978 (PR-1).
- B. *Eucommiidites* sp. (Erdtman, 1948) Hugues, 1961 (CI-1).
- C. *Eucommiidites troedssonii* (Erdtman, 1948) Hugues, 1961 (RL-1).
- D. *Arecipites microfovolatus* Ibrahim, 2002 (CI-1)



- E. *Cycadopites* sp. Wilson e Webster, 1946 (PE-1).
- F. *Dejaxpollenites foveoreticulatus* Dino, 1992 (EGST-1)
- G. *Bennettitaepollenites* sp. Thiegart, 1949 (CI-1)
- H. *Cavamonocolpites* sp. Lima, 1978 (RL-1).
- I. *Cavamonocolpites* sp.1 Dino, 1992 (CI-1) .
- J. *Clavatipollenites* sp. Couper, 1958 (EGST-1).
- K. *Clavatipollenites huguesi* Couper, 1958 (PE-1).
- L. *Stellatopollis* sp. Doyle, Van Campo e Lugardon, 1975 (VN-1).

## PLATE 10

- A. *Retimonocolpites* sp. Pierce, 1961 (PR-1).
- B. *Monocolpopollenites* sp. Thomsom & Pflug, 1953 *emend.* Nichols, Ames & Traverse, 1973 (CI-1).
- C. *Brenneripollis reticulatus* Júhasz & Góczan, 1985 (PE-1).
- D. *Afropollis jardinus* Doyle, Jardiné e Doeren Kamp, 1982 (CI-1).
- E. *Afropollis aff. jardinus* Doyle, Jardiné e Doeren Kamp, 1982 (PR-1).
- F. *Psiladicolpites papillatus* ? Regali, 1989c (EGST-1).
- G. *Tricolpites* sp. Cookson, 1947 *ex* Couper, 1953 (EGST-1).
- H. *Rousea* sp. Srivastava, 1969 (PR-1).
- I. *Rousea georgensis* (Brenner, 1963) Dettmann, 1973 (PR-1).
- J. *Trisectoris reticulatus* (Regali, Uesugui & Santos, 1974b) Heimhofer & Hochuli, 2010 (EGST-1).
- K. *Retiquadricolpites* sp. Regali, 1989 (CI-1).
- L. *Exesipollenites tumulus* Balme, 1957 (PR-1).





## PLATE 11

- A. *Cretacaeiporites* sp.? Herngreen, 1973 (RL-1).
- B. *Schizosporis* sp. Cookson e Dettmann, 1959 (PE-1).
- C. *Schizosporis parvus* Cookson e Dettmann, 1959 (RL-1).
- D. *Schizosporis spriggi* Cookson e Dettmann, 1959 (EGST-1).
- E. Acritarch Evitt 1963 (CI-1).
- F. *Cymatiosphaera* ? Wetzel, 1933 (CI-1).
- G. *Duvernaysphaera* sp. (Staplin, 1961) Deunff, 1964 (CI-1).
- H. *Maranhites* sp. Brito, 1965 *emend.* González, 2009 (CI-1).
- I. *Tasmanites* sp. Newton, 1875 *emend.* Schopf, Wilson & Bentall, 1944 (CI-1).
- J. *Scylaspora* sp. Burgess & Richardson, 1995 (EGST-1).
- K. *Raistrickia* sp.? Schopf *etal.* 1944 *emend.* Potonié & Kremp, 1954 (VN-1).
- L. *Chomotriletes* sp. Naumova, 1937 (VN-1).



PLATE 1

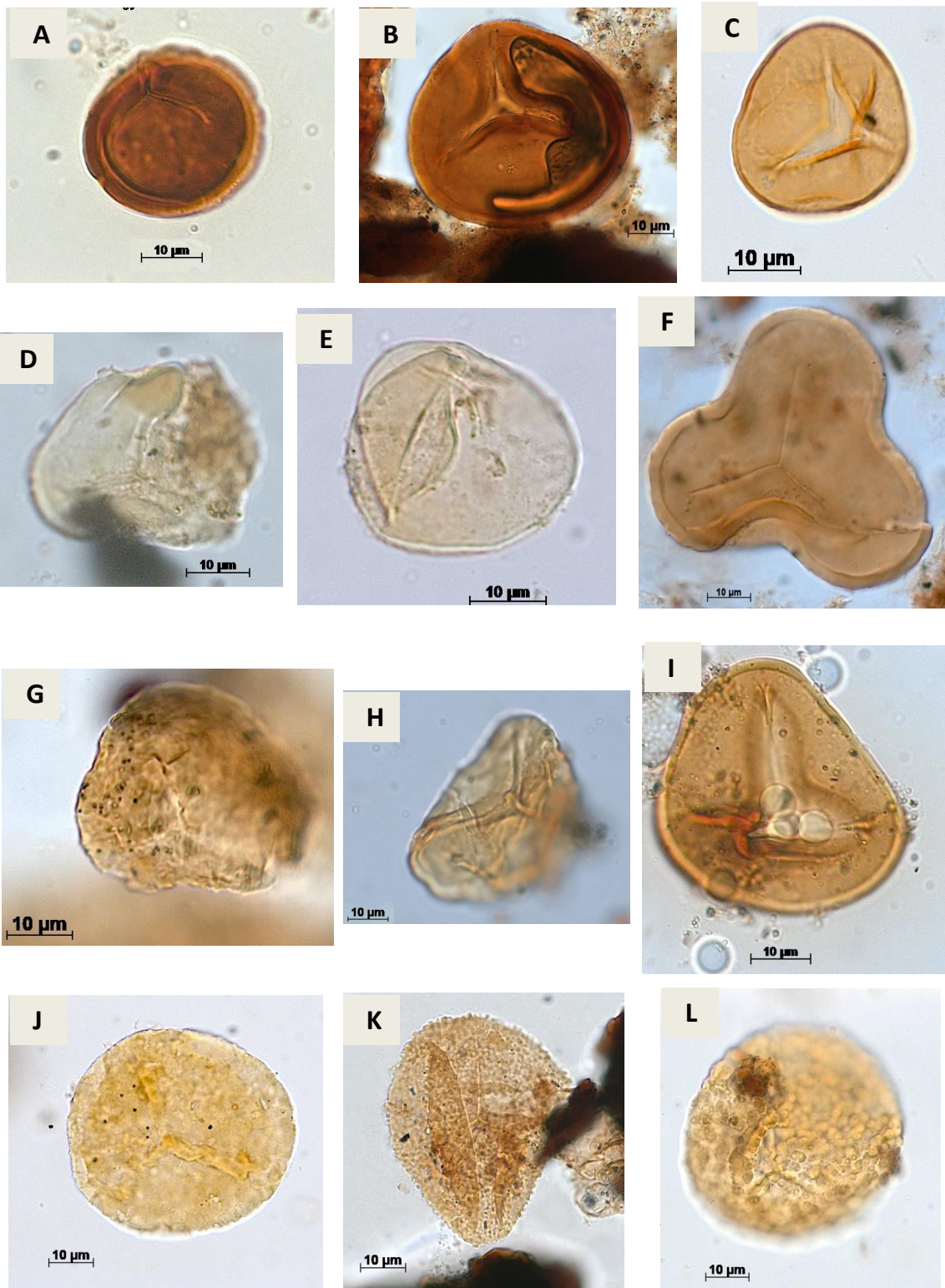




PLATE 2

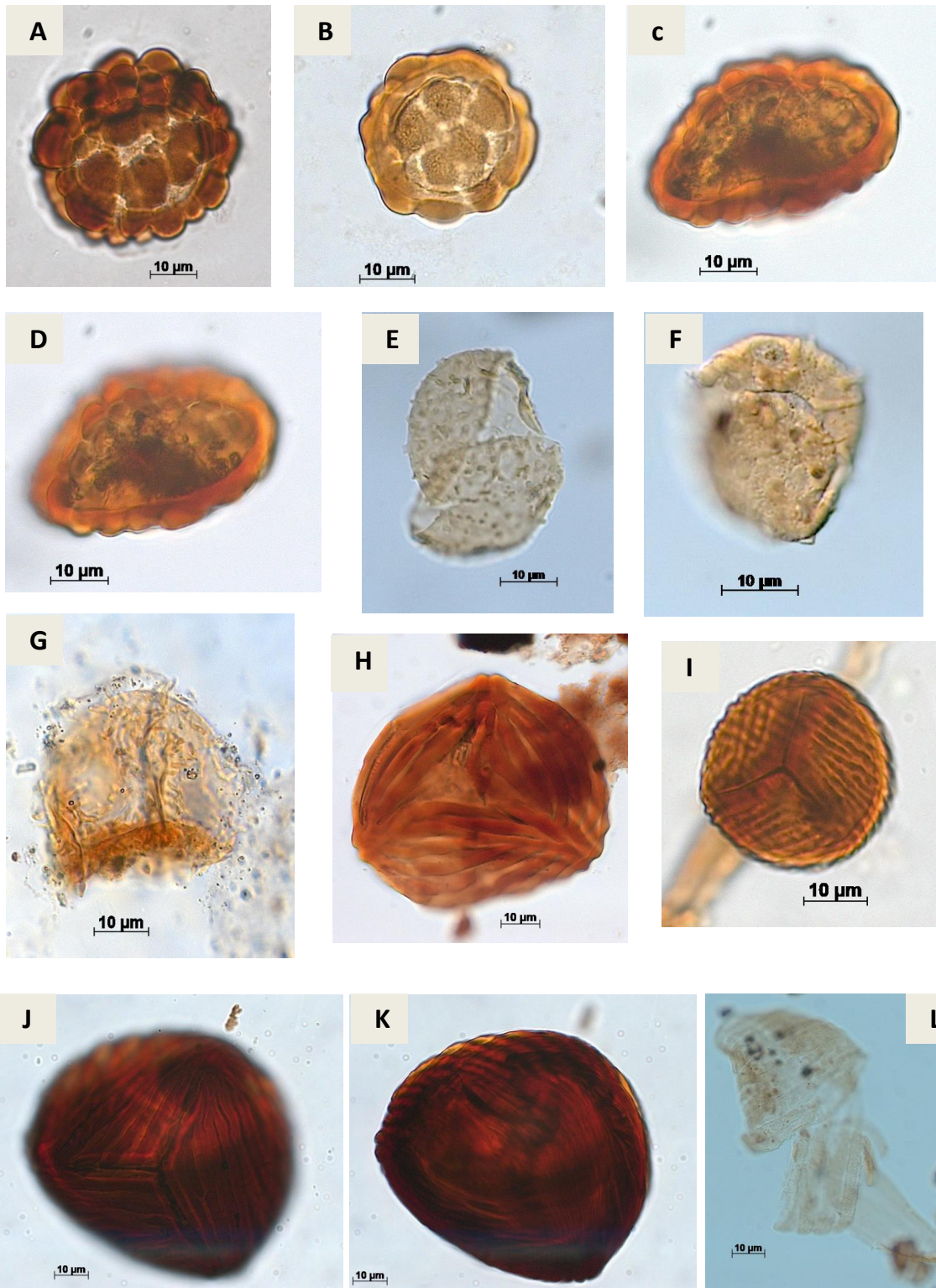






PLATE 3

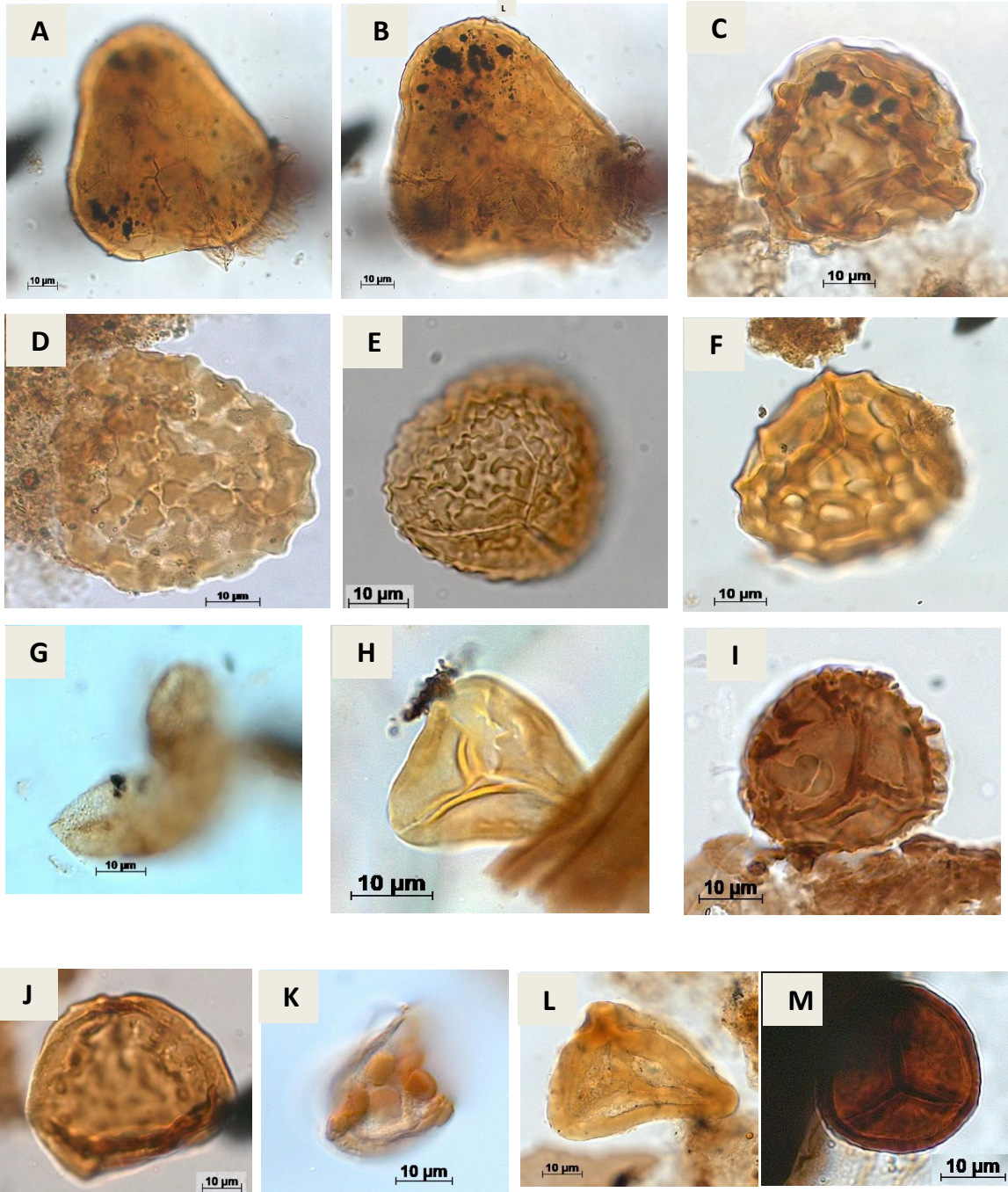




PLATE 4

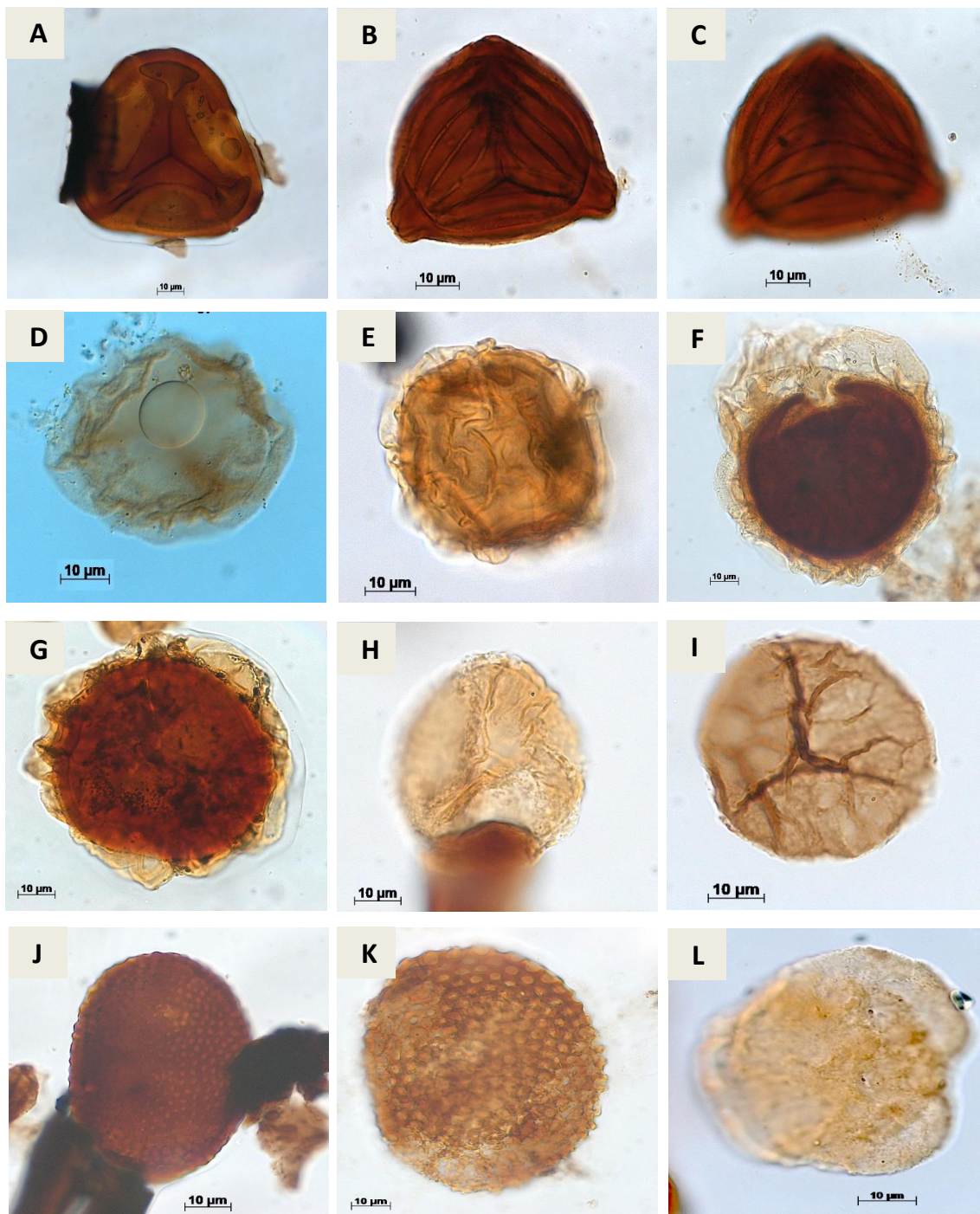






PLATE 5

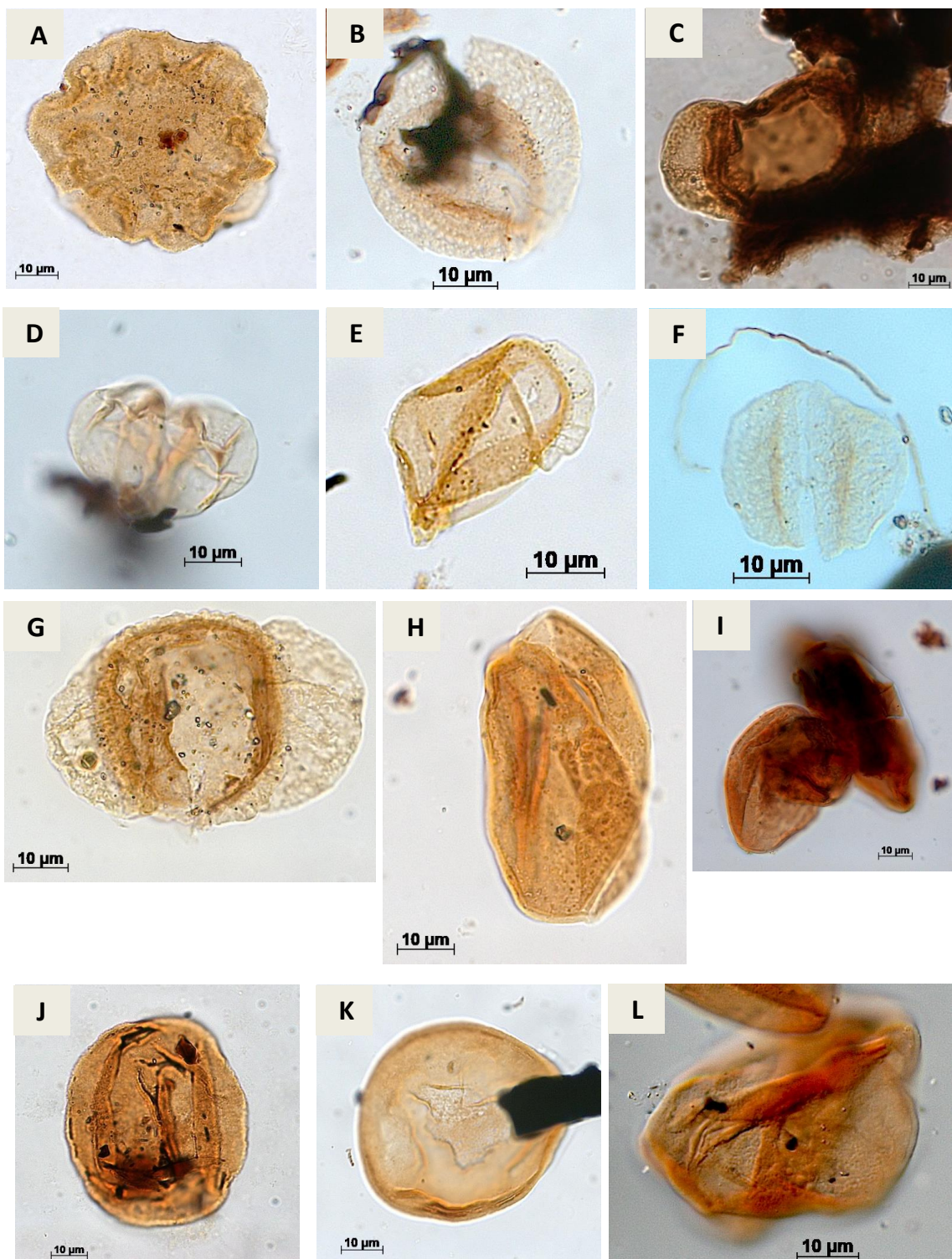




PLATE 6

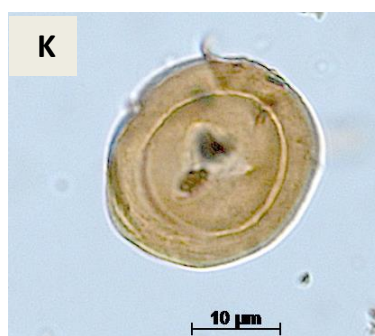
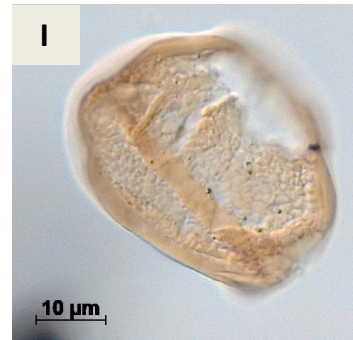
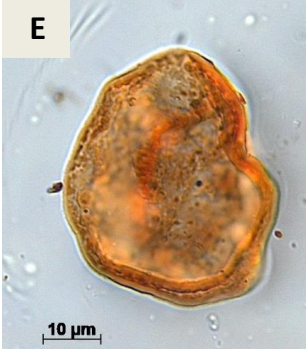
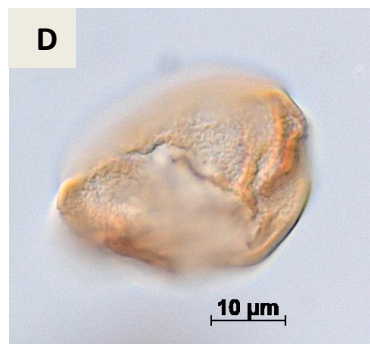
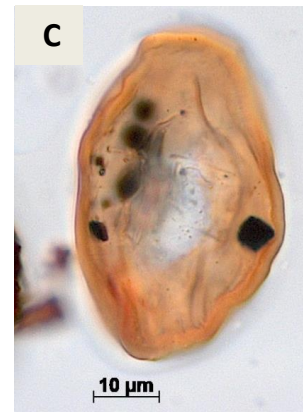
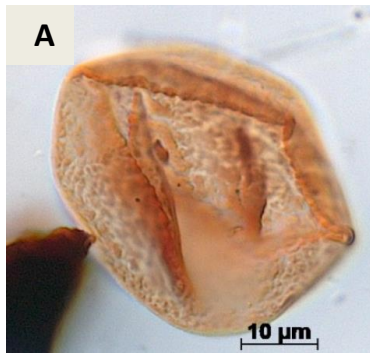






PLATE 7

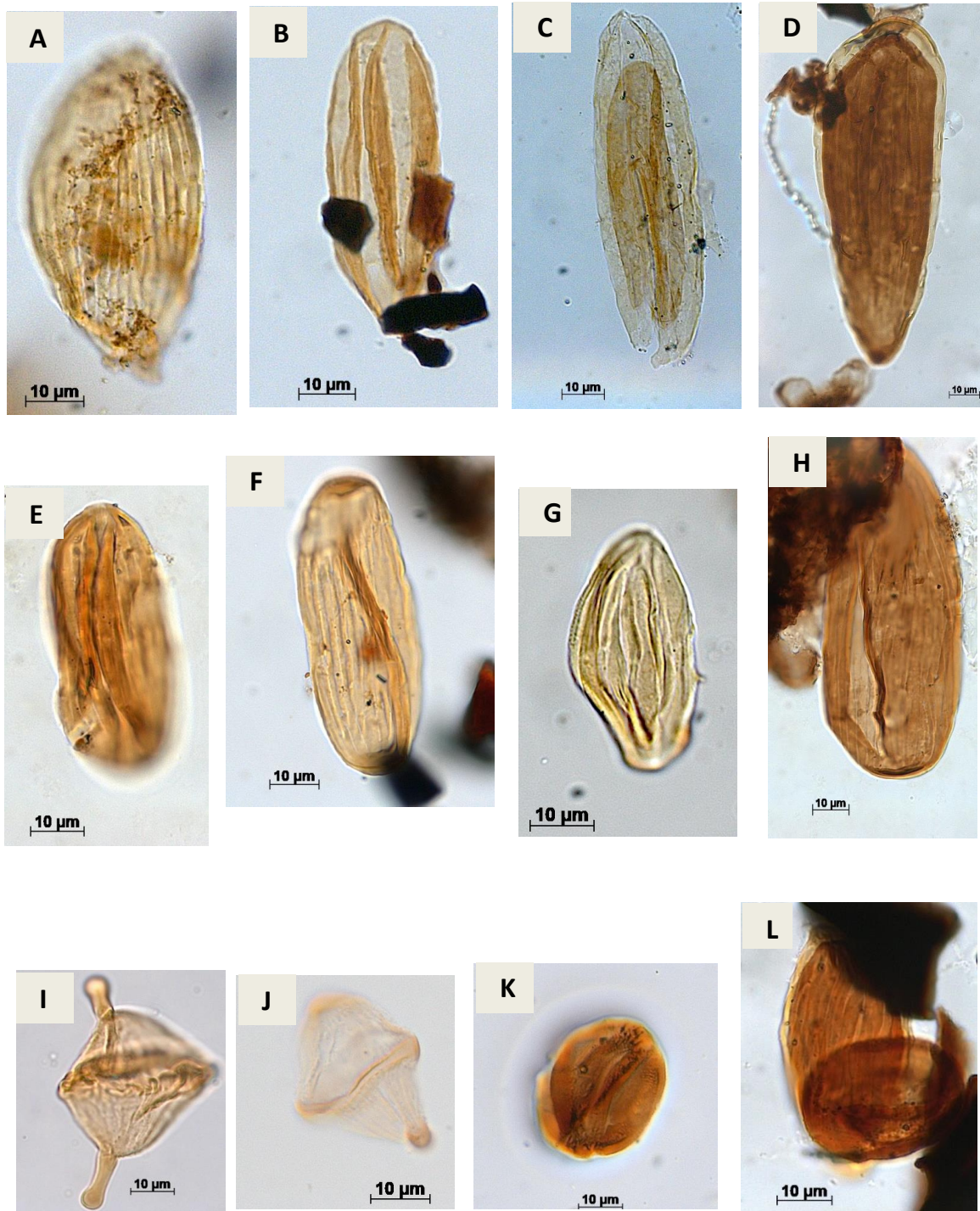






PLATE 8

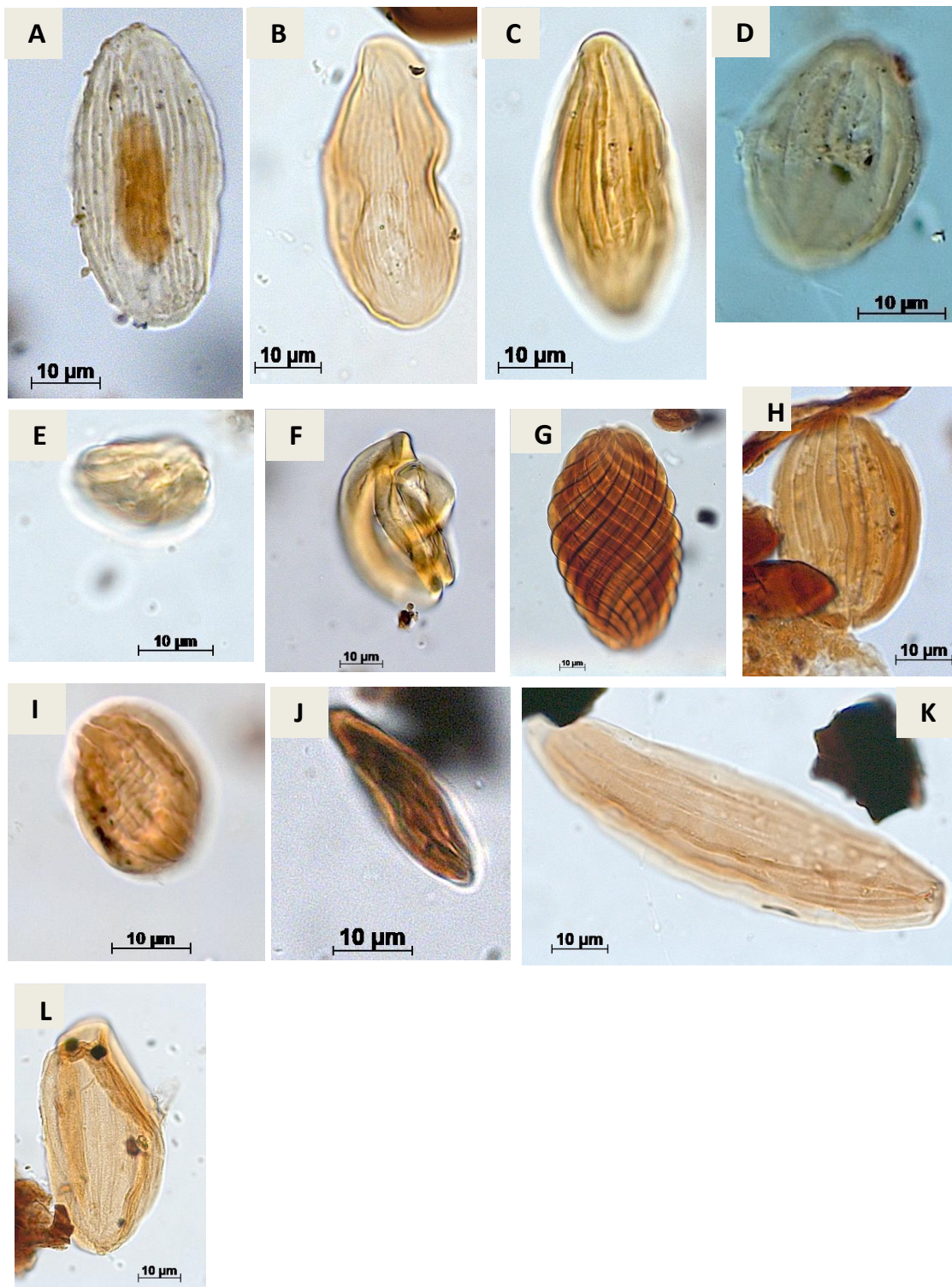




PLATE 9

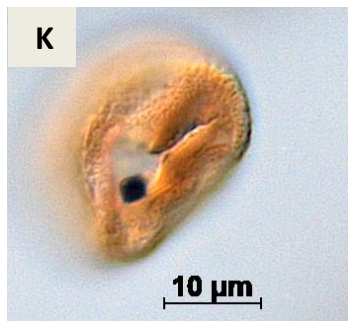
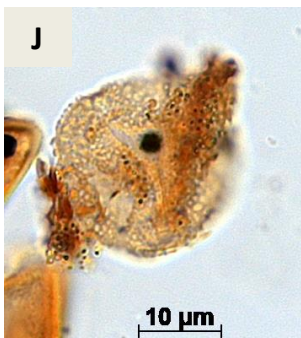
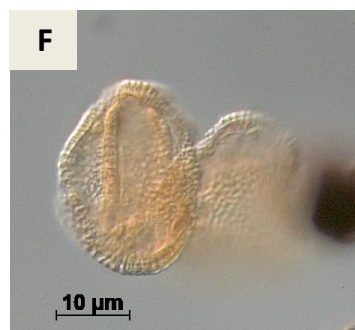
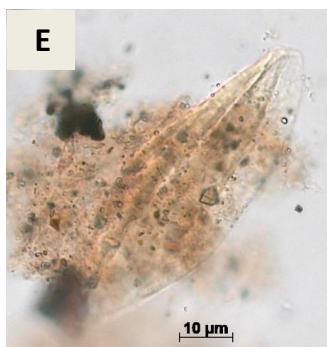
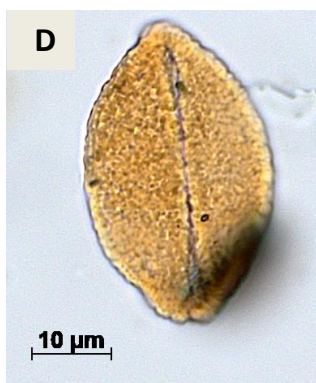
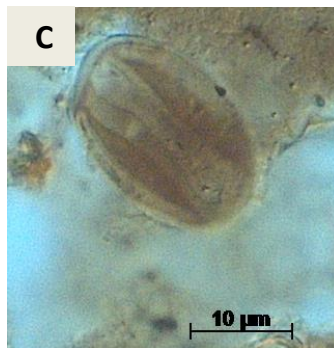






PLATE 10

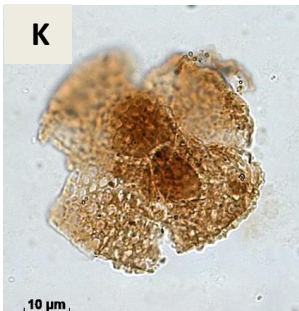
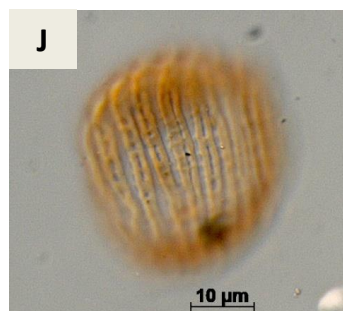
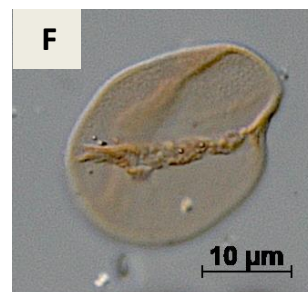
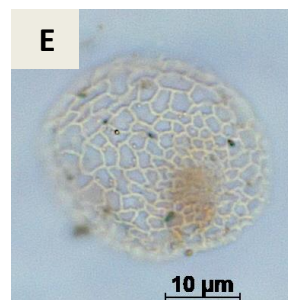
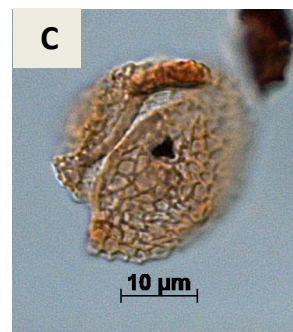
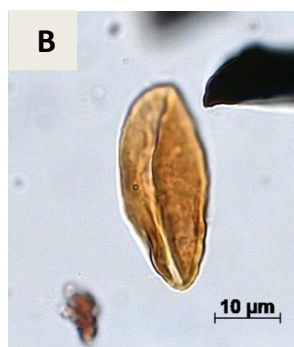
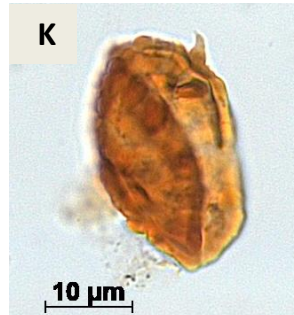
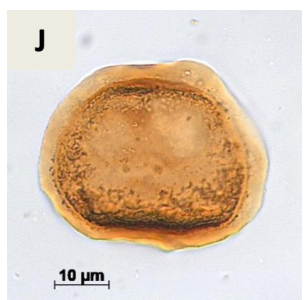
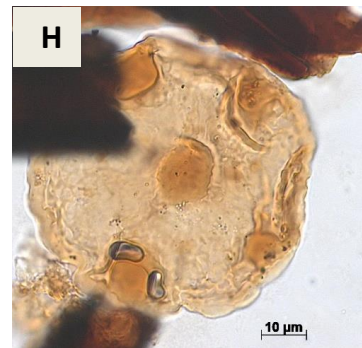
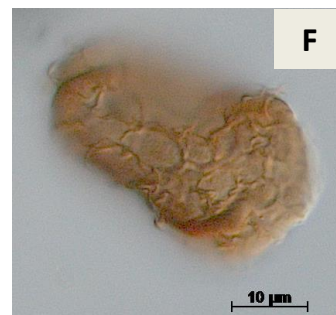
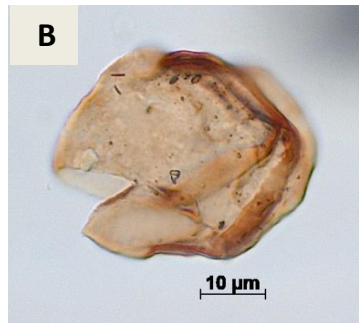
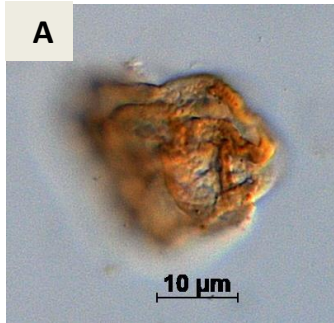




PLATE 11





Appendix 2. Bioclimatic groups (percentages) of studied wells. Legend: HG= hygrophytes; HD= hydrophytes; TLF= tropical lowland flora; UF= upland flora; XP= xerophytes; H'= diversity; Fs/X= fern spores/xerophytes.

Lithostratigraphy	Sections	Depth (m)	HG	HD	TLF	UF	XP	H'	Fs/X	Marine
Codó Formation	PR-1	1507,6	15,7	1,5	31,0	14,2	37,6	2,26	0,31	0
		1509,7	19,6	0,5	8,2	29,4	42,3	2,19	0,32	0
		1510,6	15,4	0,0	22,0	15,4	47,3	1,88	0,25	0
		1513,1	6,6	2,0	20,2	13,1	58,1	2,04	0,13	0
	PE-1	1562,0	44,4	0,0	8,7	33,2	13,8	2,59	0,76	0
		1566,0	14,4	0,6	2,2	30,0	52,8	2,21	0,22	0
		1568,5	4,2	0,0	20,8	16,7	58,3	1,99	0,07	0
		1570,0	4,1	0,0	2,4	24,1	69,4	1,90	0,06	0
	RL-1	1173,5	1,6	0,0	23,8	6,3	68,3	2,22	0,02	0
		1174,1	12,0	4,0	10,0	12,0	62,0	2,06	0,21	0
		1175,5	20,0	0,0	14,5	1,8	63,6	2,63	0,24	0
		1235,25	18,8	1,6	10,2	7,8	61,7	2,57	0,25	1
		1237,0	19,8	0,0	4,9	14,2	61,1	2,61	0,24	0
		1239,5	27,0	1,6	6,3	6,3	58,7	1,85	0,33	0
	CI-1	1240,3	11,2	0,5	13,8	5,9	68,6	1,91	0,15	0
		820,6	6,5	0,0	15,7	0,0	77,8	1,78	0,08	0
		834,5	3,7	0,0	3,7	0,0	92,6	1,30	0,04	0
		836,0	0,0	0,0	0,0	10,2	89,8	1,66	0,00	0
		837,0	14,7	2,7	6,0	48,9	27,7	2,28	0,18	0
		838,0	15,8	0,0	1,5	9,8	72,9	1,74	0,06	0
		845,0	4,8	0,0	1,4	23,3	70,5	2,07	0,33	0
		855,0	5,2	0,0	5,2	5,2	84,5	1,10	0,13	0
		855,9	10,8	0,6	10,1	3,8	74,7	2,11	0,38	0
		857,6	21,6	2,6	4,2	31,6	40,0	2,64	0,10	1
866,55		8,6	0,5	5,6	6,6	78,8	2,27	0,25	1	
866,65		16,9	1,6	4,4	21,3	55,7	2,26	0,21	0	
867,8	16,0	0,0	16,6	7,1	60,4	2,83	0,39	0		
888,75	19,3	0,0	12,9	22,9	45,0	2,28	0,30	0		
Bragança Formation	VN-1	1287,9	55,0	0,0	0,0	5,0	40,0	1,56	0,58	0
		1289,88	18,4	0,0	5,3	18,4	57,9	1,94	0,24	0
		1315,7	6,7	0,6	1,2	15,3	76,1	1,57	0,09	0
		1317,69	33,3	0,0	0,0	0,0	66,7	1,29	0,33	0
	EGST-1	676,44	19,2	0,5	14,8	54,4	11,0	2,54	0,64	0
		732,3	30,1	2,4	3,0	8,4	56,0	2,65	0,37	0
		733,3	8,1	0,0	4,3	7,6	80,0	1,48	0,09	0
		735,3	13,7	3,0	0,5	12,2	70,6	1,97	0,19	0
		1017,7	25,6	1,2	0,6	22,6	50,0	2,42	0,35	0
		1789,1	19,0	0,0	1,7	6,3	73,0	1,83	0,21	0
		1791,0	26,7	0,0	4,4	6,7	62,2	1,92	0,30	0
		1846,0	57,1	0,0	14,3	14,3	14,3	1,95	0,80	0





431 **Acknowledgements**

432 The research was funded by CENPES/PETROBRAS Grant No. 2017/00192-8 (to  
433 M.A.C.), registered by the National Petroleum Agency (ANP) as SAP 4600558879. We  
434 CENPES/PETROBRAS for the opportunity to study the data from wells, respectively,  
435 J.R. Maizatto (CENPES/PETROBRAS) for selecting wells and assistance with samples,  
436 and C. Medeiros and N. Reis (Geological Survey of Brazil—CPRM) for supporting us  
437 with infrastructure in accordance with the technical-scientific agreement  
438 (48035.000153/2020-38). We thank the A. Santos (iitOceaneon/UNISINOS) R.R.C.  
439 Ramos (Museu Nacional/UFRJ) for their helpful comments.

440

441 **Data availability**

442 The data and code used in this paper are deposited at CENPES, PETROBRAS, Rio de  
443 Janeiro, RJ, Brazil (wells VN-1, EGST-1, RL-1, PE-1, CI-1, and PR-1). Additional  
444 information on samples (wells VN-1, EGST-1, RL-1, PE-1, CI-1 and PR-1) can be  
445 accessed in [www.anp.gov.br](http://www.anp.gov.br).

446

447 **Author contributions**

448 M.C.S.G and M.A.C. led the writing with contributions of all coauthors; M.C.S.G.,  
449 C.C.L, G.S., N.P.S. and G.C.C. collected the palynological data and M.C.S.G. and  
450 M.A.C. carried out the pollen data analysis.

451

452 **Competing interests**

453 The authors declare no competing interests.



454 **References**

- 455 Antonioli L.: Estudo palinocronoestratigráfico da Formação Codó – Cretáceo Inferior  
456 do Nordeste brasileiro, PhD thesis. Universidade Federal do Rio de Janeiro, Rio  
457 de Janeiro, Brazil, 265 pp., 2001.
- 458 Balme B.E.: Spores and pollen grains from the Mesozoic of Western Australia.  
459 C.S.I.R.O, Australia, Commonwealth Scientific and Industrial Research  
460 Organization. Coal Research Section. Reference, Melbourne, T.C., 25, 1-48,  
461 1957.
- 462 Balme B.E.: Fossil in situ spores and pollen grains: an annotated catalogue. Rev.  
463 Palaeobot. Palynol., 87, 81-323, 1995.
- 464 Batten D.J.: Wealden palaeocology from the distribution of plant fossils. Proc. Geol.  
465 Ass., 85, 433-458, 1975.
- 466 Carvalho M. C., Lana C. C., Bengtson P., Sá, N. P.: Late Aptian (Cretaceous) climate  
467 changes in northeastern Brazil: A reconstruction based on indicator species  
468 analysis (IndVal). Palaeogeogr. Palaeoclimatol. Palaeoecol. 485, 553-560, 2017.
- 469 Carvalho M.A.: Palynological assemblage from Aptian/Albian of the Sergipe Basin:  
470 paleoenvironmental reconstruction. Rev. Bras. Paleontol., 7, 159-168, 2004.
- 471 Carvalho M.A., Bengtson P., Lana C.C., Sá, N.P., Santiago G., Giannerini M.C.S.: Late  
472 Aptian (Early Cretaceous) dry-wet cycles and their effects on vegetation in the  
473 South Atlantic: Palynological evidence. Cretaceous Res., 100, 172-183, 2019.
- 474 Carvalho, M.A., Bengtson, P., Lana, C.C.: Late Aptian (Cretaceous) paleoceanography  
475 of the South Atlantic Ocean inferred from dinocyst communities of the Sergipe  
476 Basin, Brazil. Paleoceanography, 31, 2–26, 2016



- 477 Carvalho, M.A., Lana, C.C., Sá, N.P, Santiago, G., Giannerini, M.C.S, Bengtson P.:  
478 Influence of the intertropical convergence zone on early Cretaceous plant  
479 distribution in the South Atlantic. *Sci. Rep.* 12, 12600, 2022.
- 480 Chaboureau, A.-C., Donnadieu, Y., Sepulchre, P., Robin, C., Guillocheau, F., Rohais,  
481 S.: The Aptian evaporites of the South Atlantic: A climatic paradox?. *Clim. Past*,  
482 8, 1047–1058, 2012.
- 483 Chaboureau, A.-C., Sepulchre, P., Donnadieu, Y., Franc, A.: Tectonic-driven climate  
484 change and the diversification of angiosperms. *PNAS* 111, 14066–14070, 2014.
- 485 Chumakov, N.M., Zharkov, M.A., Herman, A.B., Doludenko, M.P., Kalandadze, N.N.,  
486 Lebedev, E.A., Ponomarenko, A.G., Rautian, A.S.: Climate belts of themid-  
487 Cretaceous time. *Stratigr. Geol. Correl.*, 3, 241–260, 1995.
- 488 Dino R.: Palinologia, biostratigrafia e paleoecologia da Formação Alagamar- Cretáceo  
489 da Bacia Potiguar, Nordeste do Brasil, PhD. thesis, Universidade de São Paulo,  
490 Brazil, 299 pp., 1992.
- 491 Dino R.: Algumas espécies novas de grãos de pólen do Cretáceo Inferior do nordeste do  
492 Brasil. *Bol. Geociênc. Petrobras*, 8, 257-273, 1994.
- 493 Doyle J.A., Jardiné S., Dorenkamp A.: *Afropollis*, a new genus of early angiosperm  
494 pollen, with notes on the Cretaceous palynostratigraphy and paleoenvironments of  
495 northern Gondwana. *Bull. Centres Rech. Explor. Prod. Elf-Aquitaine*, 6, 39–117,  
496 1982.
- 497 Dufrêne M., Legendre, P.: Species assemblages and indicator species: the need for a  
498 flexible asymmetrical approach. *Ecol. Monogr.* 67, 345–366, 1997.
- 499 Erdtman G.: An introduction to pollen analysis. Waltham, Chronica Botanica Company,  
500 v. XII, 239 p. 1943





- 501 Erdtman G.: Handbook of Palynology: An Introduction to the Study of Pollen Grains  
502 and Spores. Copenhagen, Ejnar Munksgaard, 486 pp., 1969.
- 503 Faegri K., Iversen, J.: Textbook of Pollen Analysis. Munksgaard (Scandinavian  
504 University Books), Copenhagen, 236 Pp. 1966.
- 505 Fossilworks. <http://fossilworks.org>, last access: 27 August 2022.
- 506 Hammer O., Harper D.A.T., Ryan P.D.: PAST: paleontological statistics software  
507 package for education and data analysis. *Palaeontol. Electron.*, 4: 1-9, 2001.
- 508 Hashimoto A.T.: Contribuição ao estudo do relacionamento da palinologia e a  
509 estratigrafia de sequências. Análise da seção do Cretáceo Médio/Superior da  
510 Bacia de Santos. MSc. thesis, Universidade Federal do Rio Grande do Sul, Rio  
511 Grande do Sul, Brazil, 130 pp., 1995.
- 512 Hay W.W. and Floegel S.: New thoughts about the Cretaceous climate and oceans.  
513 *Earth-Sci. Rev.*, 115, 262-272, 2012.
- 514 Heimhofer U., Adatte T., Hochuli P.A., Burla S., Weissert H.: Coastal sediments from  
515 the Algarve: low-latitude climate archive for the Aptian—Albian. *Int. J. Earth  
516 Sci.*, 97, 785–797, 2008.
- 517 Jansonius, J., Hills, L. V. & Hartkopf-Fröder, C.: Genera File of Fossil Spores and  
518 Pollen, Spec. Pub., Department of Geology, University of Calgary, Alberta, 1976–  
519 1996.
- 520 Lima M. R.: Palinologia da Formação Santana (Cretáceo do nordeste do Brasil). II.  
521 Descrição sistemática dos esporos da Subturma Azonotriletes. *Ameghiniana*, XV,  
522 333-365, 1978.
- 523 Lima M.R.: Paleoclimatic reconstruction the Brazilian Cretaceous based on  
524 palynological date. *Rev. Bras. Geoc.*, 4, 223-228, 1983.



- 525 Lima, M. R.: Palinologia da Formação Santana (Cretáceo do nordeste do Brasil). II.  
526 Descrição sistemática dos esporos da Subturma Zonotriletes e Turma Monoletes,  
527 e dos polens das turmas Saccites e Aletes. *Ameghiniana*, XVI, 27-63, 1979.
- 528 Milani, E. J., Rangel, H. D., Bueno, G. V., Stica, J. M., Winter, W. R., Caixeta, J. M.,  
529 Neto, O. P.: Bacias sedimentares brasileiras: cartas estratigráficas. *Bol. Geoc.*  
530 *PETROBRAS*, 15, 183-205, 2007.
- 531 Ohba, M. and Ueda, H.: AGCM study on effects of continental drift on tropical climate  
532 at the early and late Cretaceous. *J. Meteorol. Soc. Jpn.* 88, 869–881, 2010.
- 533 Petri S.: Brazilian Cretaceous paleoclimates: evidence from clay-minerals, sedimentar  
534 structures and palynomorphs. *Rev. Bras. Geoc.*, 13, 215-222, 1983.
- 535 Regali M.S.P., Uesugui N., Santos A.S.: Palinologia dos sedimentos Meso-cenozoicos  
536 do Brasil (I). *Bol. Téc. Petrobras*, 17, 177-191, 1974.
- 537 Regali, M.S.P., and Santos, P.R.S.: Palinoestratigrafia e geocronologia dos sedimentos  
538 albo-aptianos das bacias de Sergipe e Alagoas – Brasil. in: *Simpósio sobre o*  
539 *Cretáceo do Brasil*, 5, Rio Claro, 1999, Rio Claro, Brazil, 411-419, 1999.
- 540 Rossetti D.F., and Góes A. M.: Caracterização paleoambiental de depósitos albianos na  
541 borda Sul da Bacia de São Luís-Grajaú: modelo de delta fluvial influenciado por  
542 tempestade. *Braz. J. Geol.*, 33, 299-312, 2003.
- 543 Santos, A., De Lira Mota, M., Kern, H.P., Fauth, G., Paim, P.S.G., Netto, R.G.,  
544 Sedorko, D., Lavina, E.L.C., Krahl, G., Fallgatter, C., Silveira, D.M., Aquino,  
545 C.D., Santos, M.O., Baecker-Fauth, S., Vieira, C.E.L.: Earlier onset of the early  
546 Cretaceous equatorial humidity belt. *Glob. Planet. Change*, 260, 103724, 2021.
- 547 Scotese, C.: A new global temperature curve for the Phanerozoic. Paper Presented at the  
548 Geological Society of America, Annual Meeting in Denver, Colorado – 287167,  
549 2016.



- 550 Scotese, C. R., Song, H., Mills, J. W. & van der Meer, D. G.: Phanerozoic  
551 paleotemperatures: The earth's changing climate during the last 540 million years.  
552 Earth Sci. Rev. 215, 10350otese, 2021
- 553 Souza-Lima, W., and Silva, R. O.: Aptian-Albian paleophytogeography and  
554 paleoclimatology from Northeastern Brazil sedimentary basins. Rev. Palaeobot.  
555 Palyno. 258, 163–189, 2018.
- 556 Suguio K., and Barcelos J. H.: Paleoclimatic evidence from the Bauru Group,  
557 Cretaceous of the Paraná Basin, Brazil. Rev. Bras. Geoc., 13, 232-236, 1983.
- 558 Uesugui N.: Palinologia: técnica de tratamento de amostras. Bol. Téc. Petrobras, 22:  
559 229-240, 1979.
- 560 Vakhrameev V.A.: Range and paleoecology of Mesozoic conifers. The  
561 Cheirolepidiaceae. Paleontol. J. 41, 11–25, 1970.
- 562 Vakhrameev V.A.: Pollen *Classopollis*: indicator of Jurassic and Cretaceous climates.  
563 Paleobotanist, 28, 301–307, 1981.

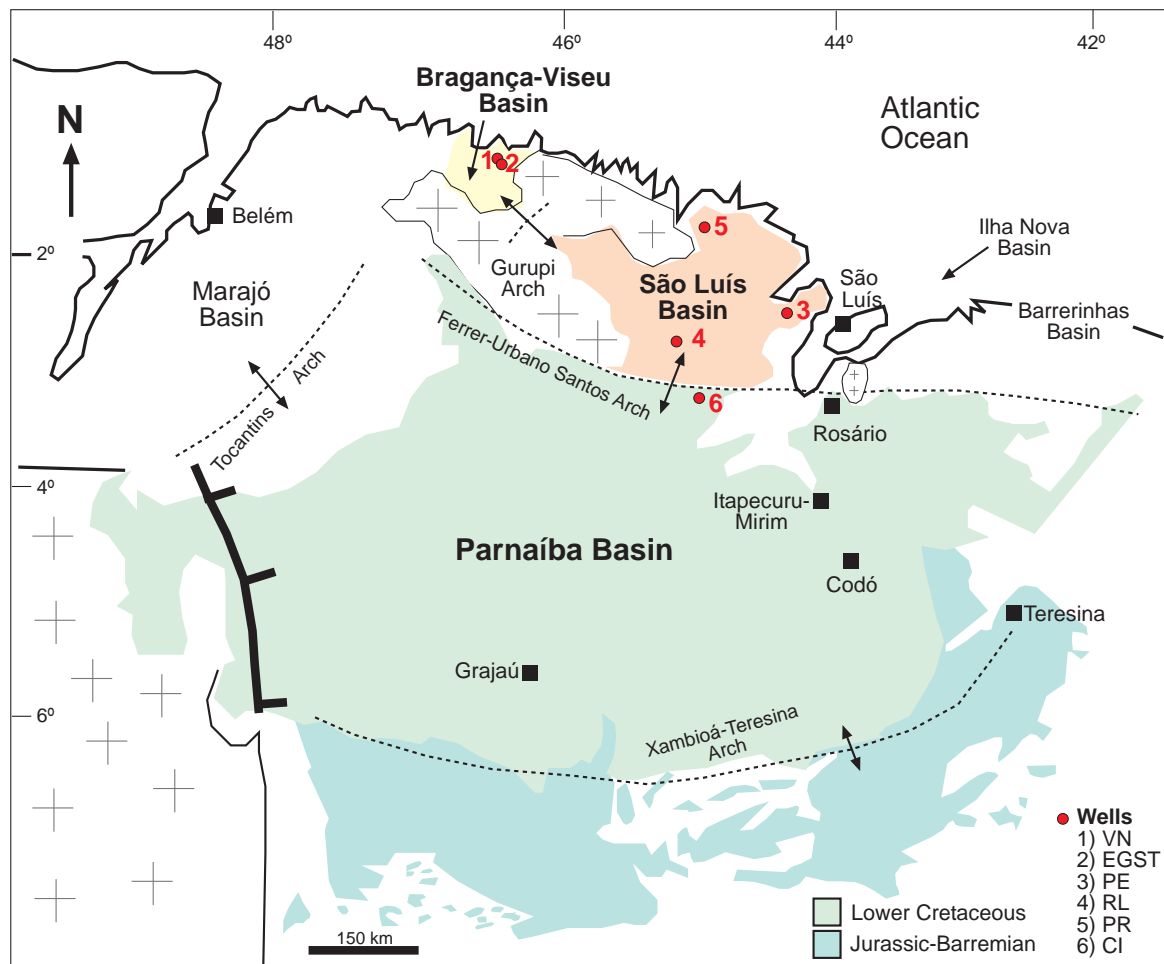
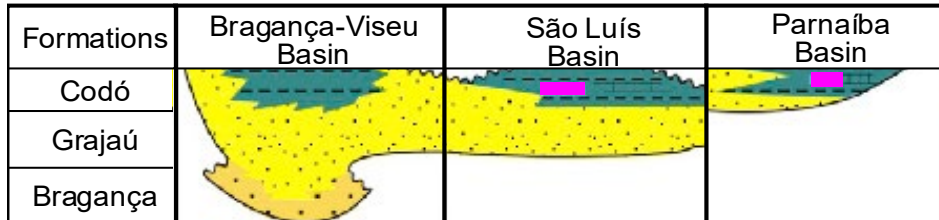


Figure 1. Location of sedimentary basins showing the sites of stratigraphic sections.



**A**



**B**

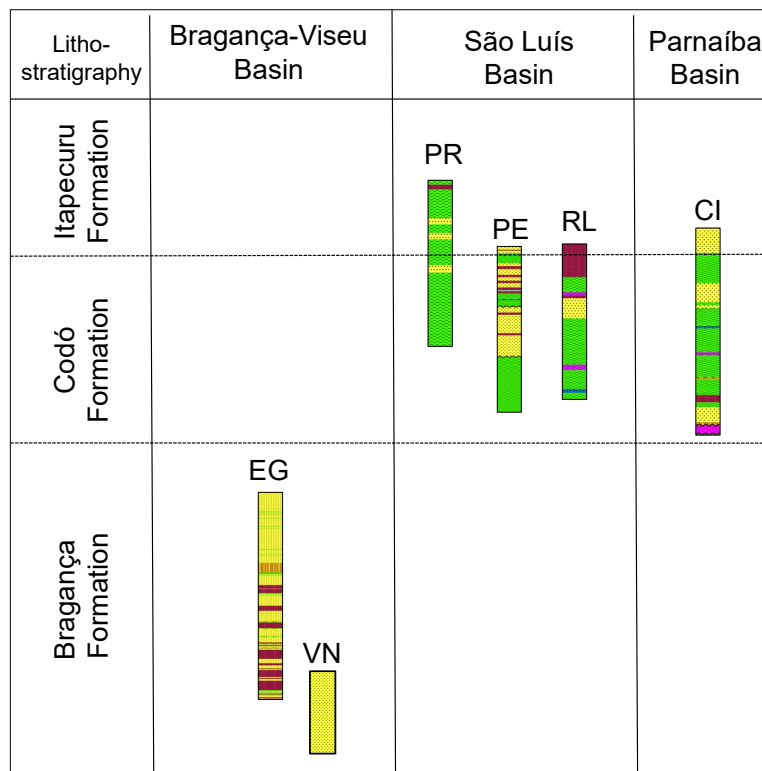


Figure 2. A) Correlation of lithostratigraphic data of the studied basins and; B) the studied wells.

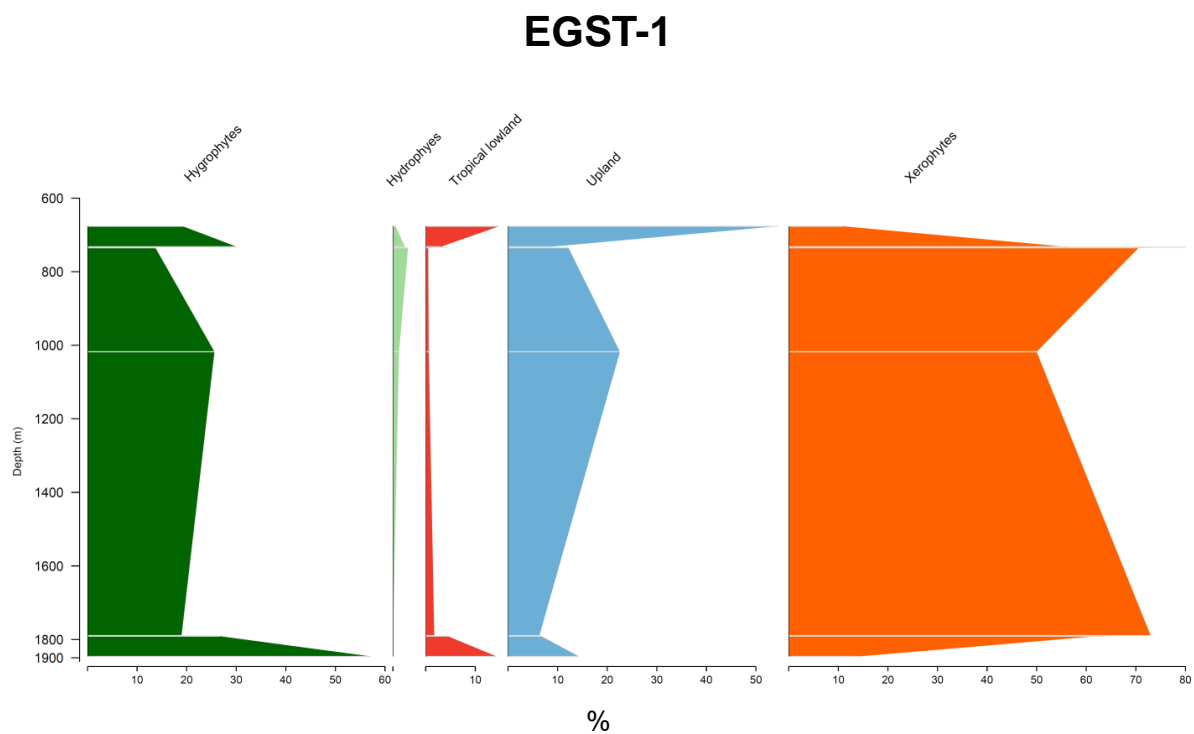


Figure 3. Stratigraphic distribution of bioclimatic groups of well EGST-1 (Bragança-Viseu Basin).

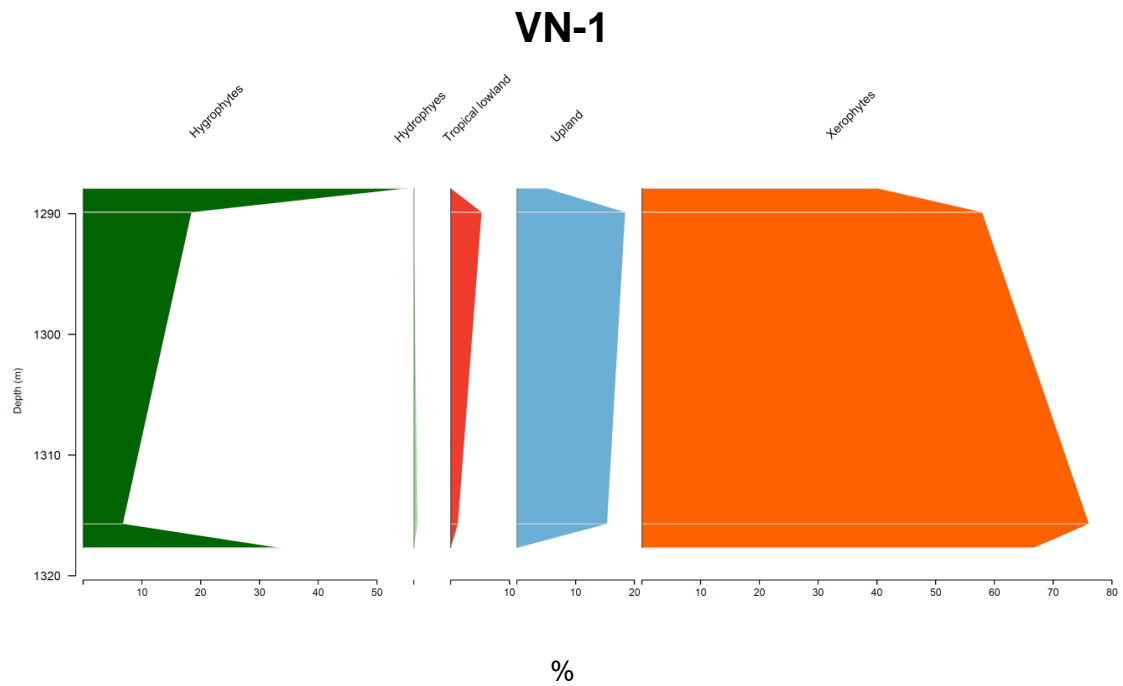


Figure 4. Stratigraphic distribution of bioclimatic groups of well VN-1 (Bragança-Viseu Basin).

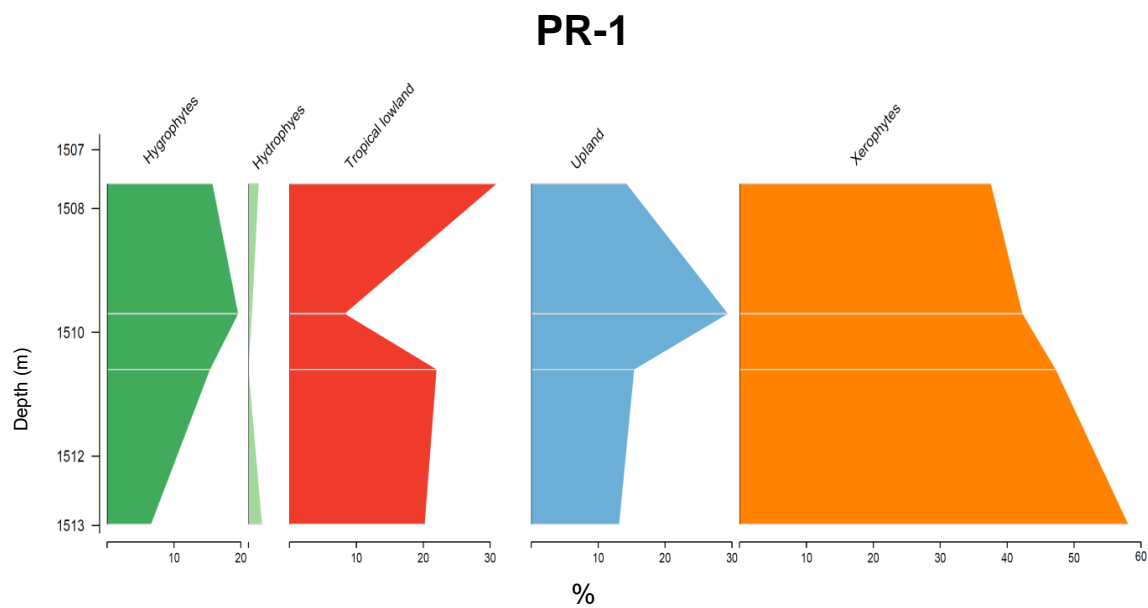


Figure 5. Stratigraphic distribution of bioclimatic groups of well PR-1 (São Luís Basin).



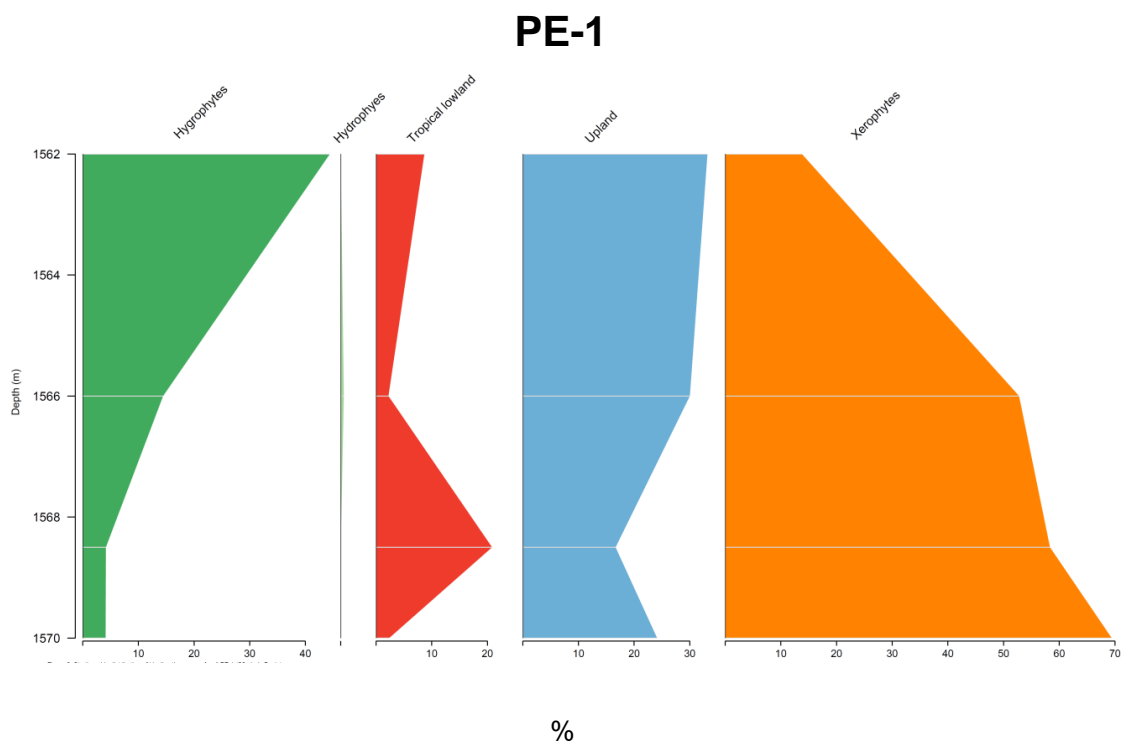


Figure 6. Stratigraphic distribution of bioclimatic groups of well PE-1 (São Luís Basin).

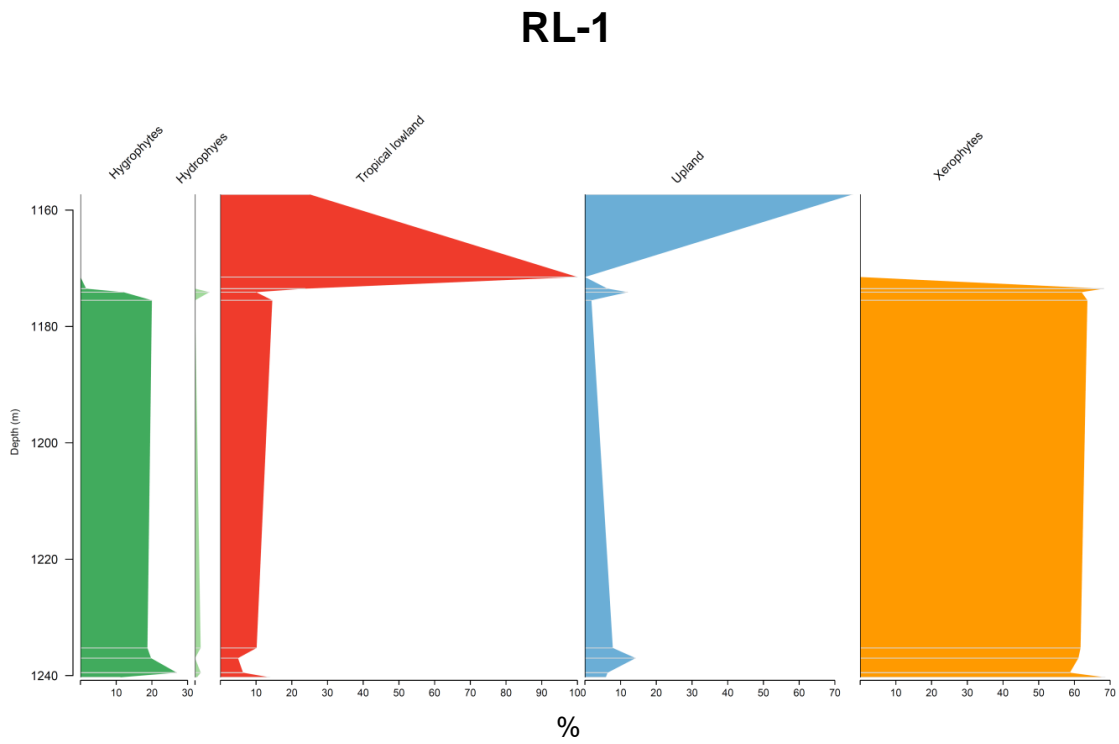


Figure 7. Stratigraphic distribution of bioclimatic groups of well RL-1 (São Luís Basin).

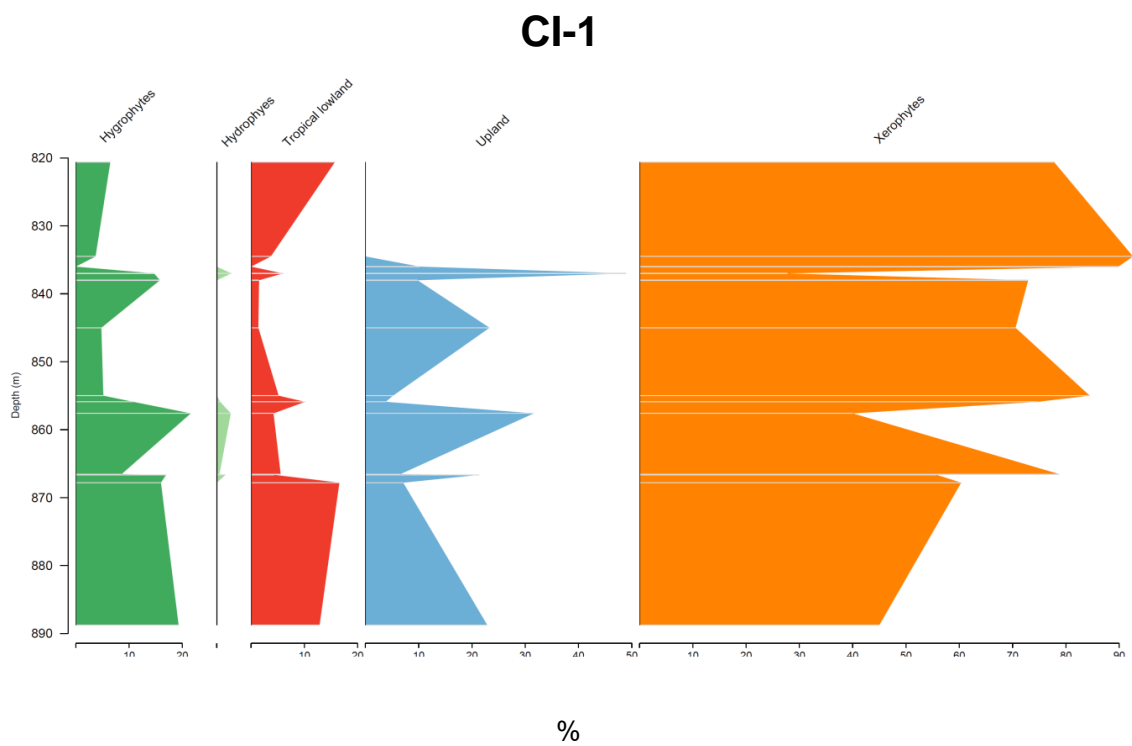


Figure 8. Stratigraphic distribution of bioclimatic groups of well CI-1 (Parnaíba Basin).

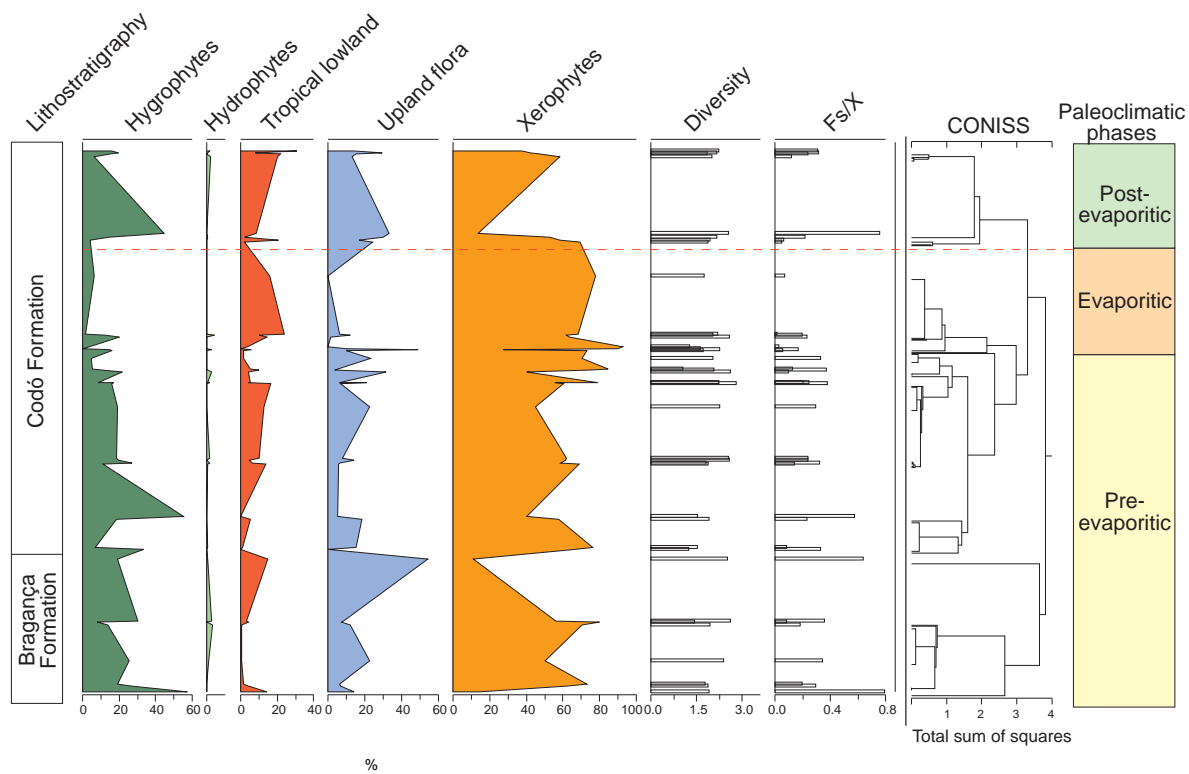


Figure 9. Composite profile showing the stratigraphic distribution of bioclimatic groups, diversity,  $Fs/X$  against the paleoclimatic phases. Agglomerative, hierarchical clustering and stratigraphically constrained dendrogram (CONISS) showing the main break (dashed red line).

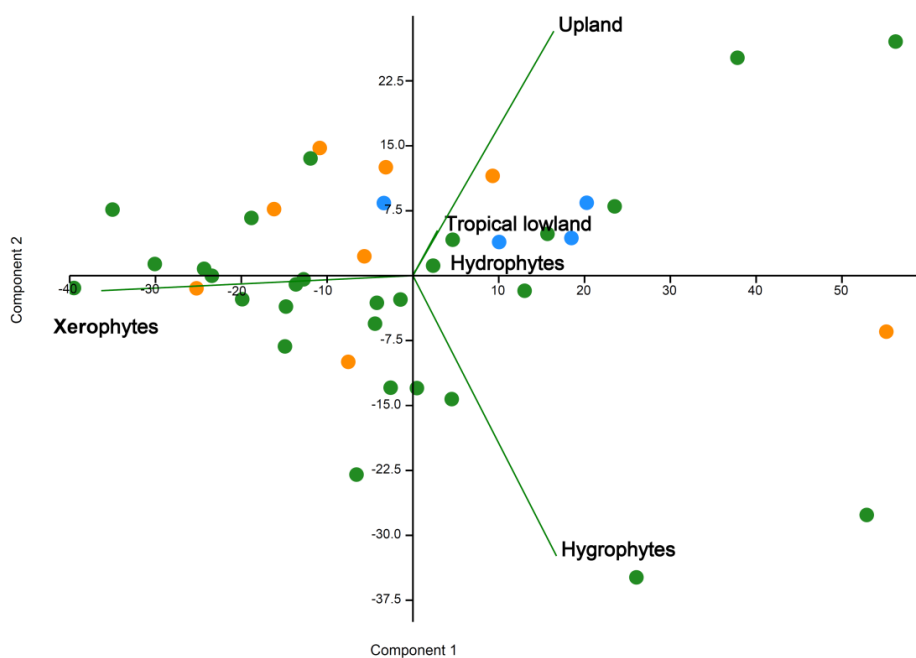


Figure 10. Principal component plot of bioclimatic groups for the pre-evaporitic phase (green dots,  $N = 28$ ), evaporitic phase (orange dots,  $N = 8$ ), and post-evaporitic phase (blue dots,  $N = 4$ ).

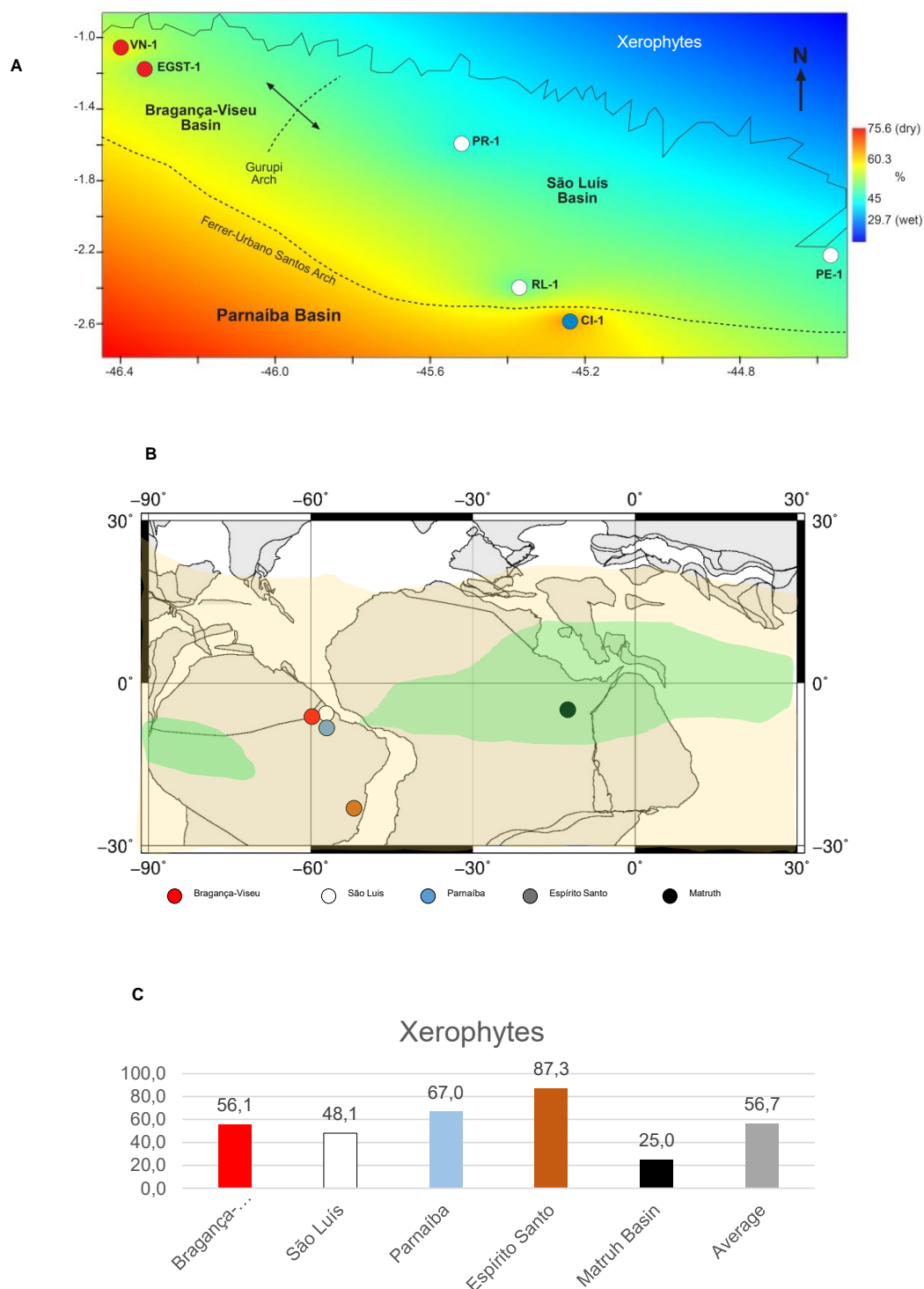


Figure 11. A) Late Aptian latitudinal distribution of the xerophyte bioclimatic group. B) Paleoclimatic belts of the late Aptian in South America (climatic belts modified from Scotese, 2016). Reconstruction map at 116 Ma modified from ODSN Plate Tectonic Reconstruction Service. C) Comparison of the bioclimatic group Xerophytes by basin. Data from the Mathru Basin (Dahab Formation) from Deaf et al. (2020).



Table 1. Localities, lithostratigraphy of the studied sections and lithologies of studied interval.

Wells	Basins	Lithostratigraphy (Formation)	Interval (m)	Lat (S)	Long (W)	No. total core samples	Lithology of the studied interval
EGST-1	Bragança-Vizeu	Bragança Fm.	676-1872.1	-01:17:55.229	-46:34:55.683	8	Sandstones, siltstones, conglomerates.
VN-1	Bragança-Vizeu	Bragança Fm.	1287.6-1317.69	-01:06:48.216	-46:40:35.673	4	Sandstones.
PE-1	São Luís	Codó Fm.	1562-1776.8	-02:22:09.725	-44:57:28.505	4	Sandstones, siltstones, calcarenites.
RL-1	São Luís	Codó Fm.	1157.3-1240.3	-02:40:21.105	-45:37:09.065	7	Sandstones, siltstones, calcarenites, anhydrites.
PR-1	São Luís	Codó Fm.	1507.6-1513.1	-01:59:59.070	-45:52:58.477	4	Sandstones, siltstones.
CI-1	Parnaíba	Codó Fm.	768-907.1	-02:59:54.215	-45:24:30.842	13	Sandstones, siltstones, conglomerates, calcarenites, anhydrites



Table 2. Plant groups, palynomorph taxa, botanical affinities and bioclimatic groups of the material studied.

Plant Groups	Palynomorph taxa	Botanical affinities	Bioclimatic groups
Bryophytes	<i>Aequitriradites</i>	Hepaticae	Hygrophyte
	<i>Cinguliriletes</i>	Sphagnaceae	Hygrophyte
	<i>Stereisporites</i>	Sphagnaceae	Hygrophyte
	<i>Triporoletes</i>	Ricciaceae	Hygrophyte
Ferns	<i>Appendicisporites</i>	Schizaeales (Anemiaceae?)	Hygrophyte
	<i>Biretisporites</i>	Osmundaceae	Hygrophyte
	<i>Cicatricosisporites</i>	Schizaeales (Anemiaceae?)	Hygrophyte
	<i>Crybelosporites</i>	Marsileaceae	Hydrophyte
	<i>Cyathidites</i>	Cyatheaceae-Dicksoniaceae	Upland flora
	<i>Deltoidospora</i>	Cyatheaceae-Dicksoniaceae	Upland flora
	<i>Distaltriangulisporites</i>	Schizaeales (Schizaeaceae?)	Hygrophyte
	<i>Foveotrilites</i>	Schizaeales (Schizaeaceae?)	Hygrophyte
	<i>Gleicheniidites</i>	Gleicheniaceae	Hygrophyte
	<i>Granulatusporites</i>	Pteridaceae	Hygrophyte
	<i>Klukisporites</i>	Schizaeales (Lygodiaceae?)	Hygrophyte
	<i>Matonisporites</i>	Matoniaceae	Upland flora
	<i>Paludites</i>	Marsileaceae	Hydrophyte
	<i>Reticulosporis</i>	Schizaeales (Schizaeaceae?)	Hygrophyte
	<i>Todisporites</i>	Osmundaceae	Hygrophyte
<i>Undulatisporites</i>	Schizaeales (Schizaeaceae?)	Hygrophyte	
<i>Verrucosisporites</i>	Osmundaceae (?)	Hygrophyte	
Lycophytes	<i>Antulsporites</i>	Selaginellaceae	Hygrophyte
	<i>Camazonosporites</i>	Lycopodiaceae	Hygrophyte
	<i>Cingulatisporites</i>	Selaginellaceae	Hygrophyte
	<i>Densoisporites</i>	Selaginellaceae	Hygrophyte
	<i>Echinatisporites</i>	Selaginellaceae	Hygrophyte
	<i>Hamulatisporis</i>	Lycopodiaceae	Hygrophyte
	<i>Leptolepidites</i>	Lycopodiaceae	Hygrophyte
	<i>Lycopodiumsporites</i>	Lycopodiaceae	Hygrophyte
	<i>Perotrilites</i>	Selaginellaceae	Hygrophyte
<i>Uvaesporites</i>	Selaginellaceae	Hygrophyte	
Pteridosperms	<i>Vitreisporites</i>	Caytoniaceae	Upland flora
Gymnosperms	<i>Araucariacites</i>	Araucariaceae	Upland flora
	<i>Balmeiopsis</i>	Araucariacites	Upland flora
	<i>Bennettitaepollenites</i>	Cycadaceae	Tropical lowland flora
	<i>Callialasporites</i>	Araucariacites/Podocarpaceae	Upland flora
	<i>Cavamonocolpites</i>	Cycadaceae	Tropical lowland flora
	<i>Cedripites</i>	Pinaceae	Upland flora
	<i>Cingulatiipollenites</i>	Araucariaceae	Upland flora
	<i>Classopollis</i>	Cheirolepidiaceae	Xerophytes
<i>Complicatisaccus</i>	Coniferae i. sedis	Upland flora	





	<i>Cycadopites</i>	Cycadaceae	Tropical lowland flora
	<i>Elateropollenites</i>	Gnetales (Gnetaceae?)	Xerophytes
	<i>Equisetosporites</i>	Gnetales (Ephedraceae?)	Xerophytes
	<i>Eucommiidites</i>	Gnetales?	Xerophytes
	<i>Exesipollenites</i>	Cupressaceae	Upland flora
	<i>Gnetaceaepollenites</i>	Gnetales (Gnetaceae?)	Xerophytes
	<i>Inaperturopollenites</i>	Cupressaceae	Upland flora
	<i>Regalipollenites</i>	Gnetales (Ephedraceae?)	Xerophytes
	<i>Rugubivesiculites</i>	Podocarpaceae	Upland flora
	<i>Sergipea</i>	Gnetales	Xerophytes
	<i>Singhia</i>	Gnetales (Ephedraceae?)	Xerophytes
	<i>Spheripollenites</i>	Cupressaceae	Upland flora
	<i>Steevesipollenites</i>	Gnetales (Gnetaceae?)	Xerophytes
	<i>Uesuguipollenites</i>	Cupressaceae	Upland flora
Angiosperms	<i>Afropollis</i>	?	Tropical lowland flora
	<i>Arecipites</i>	Monocots (Arecaceae?)	Tropical lowland flora
	<i>Brenneripollis</i>	Chloranthaceae	Tropical lowland flora
	<i>Clavatipollenites</i>	Chloranthaceae	Tropical lowland flora
	<i>Cretacaeiporites</i>	Trimeniaceae?	Tropical lowland flora
	<i>Dejaxpollenites</i>	?	Tropical lowland flora
	<i>Monocolpopollenites</i>	Monocots (Arecaceae?)	Tropical lowland flora
	<i>Psiladicolpites</i>	Monocots (Liliaceae?)	Tropical lowland flora
	<i>Retimonocolpites</i>	Monocots (Arecaceae?)	Tropical lowland flora
	<i>Retiquadricolpites</i>	?	Tropical lowland flora
	<i>Rousea</i>	Eudicots (Flacourtiaceae?)	Tropical lowland flora
	<i>Stellatopolis</i>	?	Tropical lowland flora
	<i>Tricolpites</i>	Eudicots	Tropical lowland flora
	<i>Trisectoris</i>	Illiciaceae	Tropical lowland flora



Table 3. Description of the bioclimatic groups and their main representatives.

Bioclimatic groups	Main representatives (sporomorph genera)	Remarks
Hydrophytes	<i>Crybellosporites</i>	Hydrophytes represent aquatic plants that live with a portion of their vegetative parts permanently immersed in water.
Hygrophytes	<i>Cicatricosisporites</i>	Hygrophyte plants depend on water to reproduce and are therefore generally associated with moist conditions and rarely reported from arid environments.
Tropical lowland flora	<i>Afropollis</i>	The tropical lowland flora is composed by families related to more humid conditions in lowland areas. All angiosperm genera and morphotypes are included in this flora
Upland flora	<i>Araucariacites</i> , <i>Caliallasporites</i>	Families assigned to thermophilic, large conifers, formed forests in the highlands from 200 to 1800 m.
Xerophytes	<i>Classopollis</i> , <i>Gnetaceaepollenites</i>	The group is adapted to xeric or water-stressed environments and therefore associated with arid climates.



Table 4. Average abundance of bioclimatic groups, diversity ( $H'$ ) and Fs/X ratio of the studied wells.

Basins	Wells	Hydrophytes	Hygrophytes	Tropical lowland flora	Upland flora	Xerophytes	Fs/X	$H'$
Bragança-Viseu	EGST-1	0.9	24.9	5.5	16.6	52.1	0.38	2.1
Bragança-Viseu	VN-1	0.2	28.4	1.6	9.7	60.2	0.31	1.6
São Luís	PR-1	1.0	14.3	20.4	18.0	46.3	0.25	2.1
São Luís	PE-1	0.1	16.8	8.5	26.0	48.6	0.28	2.2
São Luís	RL-1	1.0	15.8	12.0	7.8	63.4	0.24	1.9
Parnaíba	CI-1	0.7	11.4	6.0	15.9	63.6	0.19	2.0
<i>General average</i>		<i>0.7</i>	<i>18.6</i>	<i>9.0</i>	<i>15.7</i>	<i>55.7</i>	<i>0.28</i>	<i>2.0</i>



Table 5. Average abundance of bioclimatic groups, diversity, Fs/X and marine elements of the paleoclimatic phases for the Bragança-Viseu, São Luís and Parnaíba basins. No marine elements.

Paleoclimatic phases	Hygrophytes	Hydrophytes	Tropical lowland flora	Upland flora	Xerophytes	Diversity (H')	Fs/X	IndVal
Pre-evaporitic	18.8	0.7	5.6	14.1	60.7	2.0	0.3	<i>Deltoidospora</i> sp. (80.6%)
Evaporitic	10.0	1.0	16.0	5.0	67.9	2.2	0.1	<i>Afropollis</i> spp. (79.3%)
Post-evaporitic	15.5	0.6	14.4	22.0	47.4	2.1	0.3	<i>Deltoidospora</i> sp. (86.2%)
<i>General average</i>	<i>14.8</i>	<i>0.8</i>	<i>12.0</i>	<i>13.7</i>	<i>58.7</i>	<i>2.1</i>	<i>0.2</i>	